Changes in atmospheric moisture transport over tropical South America: an analysis under a climate change scenario

Paola A. Arias[1] · Maria Lizeth Rendón[1] · J. Alejandro Martínez[2] · Richard P. Allan[3]

Abstract

Warming induced by increased greenhouse gas emissions is intensifying the global water cycle and increasing the water vapor content of the global atmosphere. However, there is a lack of scientific literature assessing how regional atmospheric moisture transport and recycling will change in a warming climate. This work analyzes the projections of atmospheric moisture transport and recycling over tropical South America by the end of the twenty-first century (2070–2100) under a climate change scenario (RCP8.5). We used the Dynamic Recycling Model to estimate atmospheric moisture contributions to the region considering input data from the European Centre for Medium-Range Weather Forecasts ERA5 reanalysis and 11 models included in the Fifth Phase of the Coupled Model Intercomparison Project. Projected increases of precipitable water in tropical South America are linked with increased evaporation from the oceans. However, those projections also indicate (1) reductions in the precipitation contributed by the main atmospheric moisture sources to the continental regions of tropical South America, (2) reductions of total precipitation, and (3) reductions of recycled precipitation over the region. The largest reductions of precipitation recycling are projected over the southern Amazon during the dry-to-wet transition season (about 31%) and the northern Amazon during its dry season (about 25%). This is particularly relevant since the southern Amazon has experienced the occurrence of longer dry seasons during the recent decades and has been highlighted as a hotspot of climate change.

Keywords Atmospheric moisture transport · Moisture recycling · Northern South America · Amazon · Climate change

1 Introduction

It is unequivocal that human influence has warmed the atmosphere, ocean and land (IPCC 2021). As a consequence, the global water cycle has experienced substantial and widespread changes since the mid-twentieth century, particularly an intensification since at least 1980, with increased atmospheric moisture fluxes and amplified precipitation minus evaporation patterns (Arias et al. 2021a; Douville et al. 2021). A warmer climate increases water vapor transport

into weather systems, making wet seasons and events wetter, but also drives an increase in the atmospheric evaporative demand and the severity of droughts (Douville et al. 2021). As a consequence, weather and climate extremes, such as heavy precipitation and drought, are increasing in frequency and intensity over many regions (IPCC 2021; Seneviratne et al. 2021).

Global atmosphere moisture has increased since the 1980s, with increases of near-surface specific humidity over both ocean and land since at least the 1970s (Willett et al. 2014, 2020; Douville et al. 2021; Allan et al. 2022). However, the regional atmospheric circulation strongly influences the regional climate response, with water vapor transport and moisture recycling playing an important role. Although the Sixth Assessment Report (AR6) of the Intergovernmental Panel on Climate Change (IPCC) assesses high confidence on an increase of global atmospheric moisture transport due to human activity (Douville et al. 2021), there is a lack of scientific literature assessing how regional atmospheric moisture transport and recycling is changing and will

✉ Paola A. Arias
    paola.arias@udea.edu.co

1   Grupo de Ingeniería Y Gestión Ambiental (GIGA),
    Escuela Ambiental, Facultad de Ingeniería, Universidad de
    Antioquia, Medellin, Colombia

2   Escuela Ambiental, Facultad de Ingeniería, Universidad de
    Antioquia, Medellin, Colombia

3   Department of Meteorology and National Centre for Earth
    Observation, University of Reading, Reading, UK

continue changing as a consequence of increased human-caused GHG, particularly for tropical South America.

Previous studies have identified the climatological behavior of water vapor transport over tropical South America. Numerical models of different levels of complexity have been widely used to identify aspects related to: (1) the main moisture sources for the region (e.g. Drumond et al. 2008; Sakamoto et al. 2011; Arias et al. 2015a, b; Hoyos et al. 2018; Sorí et al. 2018; Nieto et al. 2019; Escobar et al. 2022), (2) the interannual variations of the regional atmospheric moisture transport (e.g. Hoyos et al. 2019; Morales et al. 2020), (3) the diurnal cycle of the water vapor contributions to the region (Zahn and Allan 2013; Dominguez et al. 2022), (4) the role of the low-level jets (Poveda et al. 2014; Arias et al. 2015a, b; Gimeno et al. 2016; Gallego et al. 2019; Morales et al. 2020), (5) the variations of the regional patterns of atmospheric moisture transport related to land cover changes (Agudelo et al. 2019; Molina et al. 2019; Ruiz-Vásquez et al. 2020; Sampaio et al. 2021; Ruv Lemes et al. 2023), and (6) the relative contributions of recycled humidity (e.g. Bosilovich and Chern 2006; Zemp et al. 2014; Staal et al. 2018; Dominguez et al. 2022; Escobar et al. 2022) and moisture advection from the oceans (Gimeno et al. 2012, 2020). Moreover, recent studies have provided isotopic evidence that confirm the importance of continental moisture sources over the region, like the Amazon (Ampuero et al. 2020) or the Orinoco basin (Escobar et al. 2022).

Particularly, water vapor recycling and transport in the Amazon has received special attention in the literature. Different studies show that the Amazon basin receives atmospheric moisture advected from the South Atlantic and the North Atlantic (e.g. Bosilovich and Chern 2006; Drumond et al. 2008, 2014; Satyamurty et al. 2013; Rocha et al. 2017; Sori et al. 2018; Agudelo et al. 2019). The relevant role of atmospheric moisture recycling over the southern Amazon has been also widely addressed (e.g. Zemp et al. 2014; Swann et al. 2015; Marengo et al. 2017; Rocha et al. 2017; Staal et al. 2018; Ampuero et al. 2020; Ruiz-Vásquez et al. 2020; Tuinenburg et al. 2020; Dominguez et al. 2022). Given the importance of moisture recycling in the Amazon, several studies have focused on the impacts of deforestation and land cover change in this region on water vapor recycling and transport (Agudelo et al. 2019; Molina et al. 2019; Ruiz-Vásquez et al. 2020; Sampaio et al. 2021; Ruv Lemes et al. 2023). However, few studies focus on the projected changes of atmospheric moisture transport over the Amazon, and tropical South America in general, in association with human-induced climate change.

Therefore this work aims to analyze the projections of atmospheric moisture transport and recycling over tropical South America under a climate change scenario. We used the Dynamic Recycling Model (DRM; Dominguez et al.

2006) to estimate atmospheric moisture contributions to the region considering input data from the European Centre for Medium-Range Weather Forecasts (ECMWF) ERA5 reanalysis (Hersbach et al. 2020) and 11 models included in the Fifth Phase of the Coupled Model Intercomparison Project (CMIP5; Taylor et al. 2012). In particular, we considered projections by the end of the twenty-first century (2070–2100) under the Representative Concentration Pathway (RCP) with the highest GHG concentrations—RCP8.5 (Riahi et al. 2011). We used the RCP8.5 since this provides a greater signal for understanding projected changes in water vapor transport while lower emission scenarios produce similar but smaller responses. With this analysis, we aim to contribute to the understanding of regional climate change over tropical South America, a region with high vulnerability to climate change (Castellanos et al. 2022).

2 Data and methodology

2.1 Reanalysis data

We used hourly fields of precipitation, evaporation, precipitable water, and vertically integrated horizontal moisture fluxes (WIMF) for zonal and meridional directions from the ERA5 reanalysis (Hersbach et al. 2020) during the period 1980–2005. We estimated daily means from the hourly data to run the DRM. In ERA5, evaporation corresponds to the accumulated amount of water that has evaporated from the Earth's surface, including a simplified representation of transpiration (from vegetation), into vapour in the air above. ERA5 is the most recent reanalysis of the ECMWF, with a 30 km horizontal grid size and 137 pressure levels. Extensive conventional in-situ measurements and satellite observations, including those sampling surface and tropospheric humidity, are combined with a high-resolution atmosphere modeling system using four dimensional-variational data assimilation. Precipitation and evaporation are not assimilated variables over the region and are instead generated by the model that will introduce biases. However, the simulation is expected to be realistic given the assimilation of determinant variables such as temperature and water vapor and as demonstrated in evaluation against observations (e.g., Hersbach et al. 2020; Watters et al. 2021; Eiras-Barca et al. 2022). This product is the state-of-the-art reanalysis used in studies focused in water vapor tracking (Tuinenburg and Staal 2020).

2.2 CMIP5 model outputs

This work also uses CMIP5 outputs for daily fields of surface latent heat flux, precipitation, zonal and meridional winds and specific humidity at different pressure levels from

11 CMIP5 models (Table 1). Since the variable evaporation is not available from the CMIP5 models considered, we used surface latent heat flux to estimate evaporation. Latent heat flux is converted from an energy flux to a moisture flux using the latent heat of vaporization. This includes evaporation from bare ground and water bodies as well as evaporation from intercepted water on vegetated surfaces and transpiration from vegetation.

We selected these models based on the availability of daily data for the historical and RCP8.5 runs, which is required to run the DRM. A larger set of models, including the CMIP6 set, were not considered here since the full set of diagnostics were not available. Thus, a representative set of CMIP5 models was used while noting that the full range of responses across CMIP5 and CMIP6 would provide a fuller but not necessarily complete range of plausible responses that could be investigated in future studies.

We considered historical runs for the period 1980–2005. Historical simulations include all forcing observed during the twentieth century (1850–2005), including changes in the atmospheric composition due to human activities, volcanic eruptions, land use changes, solar forcing and aerosol emissions (Taylor et al. 2012). In addition, we considered twenty-first century projections under the RCP8.5 scenario for the period 2070–2100. The RCP8.5 corresponds to the scenario with the highest GHG emissions amongst the four RCPs introduced in the AR5, reaching a CO2-equivalent (CO2-eq) concentration of 1370 ppm and a radiative forcing of 8.5 W/m^2 by 2100 (Riahi et al. 2011). The spatial land cover considerations of the RCP8.5 include: (1) built-up land (residential plus infrastructure), (2) cultivated land (arable and permanent crops, separated by irrigated and non-irrigated land), (3) forests (separated by managed and unmanaged forests), (4) grassland/woodland/shrubland (GWS), and (5) other land (water, desert, rocks, and ice). Major improvements of the RCP8.5 include updates with respect to the representation of base-year land-cover statistics and updates in inventories. The RCP8.5 also considers the split of the aggregated GWS category into pasture and natural grasslands, which was done specifically to represent dynamic land-cover changes in climate projections (Riahi et al. 2011).

Although the RCP8.5 is a very high GHG emissions scenario, the robust scaling of atmospheric moisture with temperature mean that results are expected to apply to lower emissions scenarios with a lower magnitude response, while it provides the benefit of maximizing the signals of interest. In addition, climate sensitivity varies across models, thereby also providing a range of warming pathways for each scenario.

2.3 Atmospheric moisture transport

We used the DRM to track the water vapor originating from different source regions and transported to sink regions in tropical South America. The DRM is a 2D analytical model that uses a semi-Lagrangian approach to estimate the spatio-temporal variation of the atmospheric moisture that is recycled in a target region (i.e., that originates as evapotranspiration in the same region) and is advected to and from other remote regions (Dominguez et al. 2006; Martinez and Dominguez 2014). The model is derived from the water vapor conservation equation integrated into the

Table 1 General description of the 11 CMIP5 models used

Model	Institute	Lon×Lat resolution	Type	References
CanESM2	Canadian Centre for Climate Modeling and Analysis	2.8°×2.8°	ESM	Arora et al. (2011)
GFDL-CM3	NOAA/Geophysical Fluid Dynamics Laboratory	2.5°×2.0°	AOGCM	Donner et al. (2011)
GFDL-ESM-2G	NOAA/Geophysical Fluid Dynamics Laboratory	2.5°×2.0°	ESM	Donner et al. (2011)
GFDL-ESM-2M	NOAA/Geophysical Fluid Dynamics Laboratory	2.5°×2.0°	ESM	Donner et al. (2011)
MIROC5	Atmosphere and Ocean Research Institute (The University of Tokyo), National Institute for Environmental Studies, and Japan Agency for Marine-Earth Science and Technology	1.4°×1.4°	AOGCM	Watanabe et al. (2010)
MIROC-ESM	Atmosphere and Ocean Research Institute (The University of Tokyo), National Institute for Environmental Studies, and Japan Agency for Marine-Earth Science and Technology	2.8°×2.8°	ESM	Watanabe et al. (2010)
MIROC-ESM-CHEM	Atmosphere and Ocean Research Institute (The University of Tokyo), National Institute for Environmental Studies, and Japan Agency for Marine-Earth Science and Technology	2.8°×2.8°	ESM	Watanabe et al. (2010)
MPI-ESM- MR	Max Planck Institute for Meteorology	1.9°×1.9°	ESM	Zanchettin et al. (2013)
MRI-CGCM-3	Meteorological Research Institute	1.1°×1.1°	AOGCM	Yukimoto et al. (2012)
MRI-ESM1	Meteorological Research Institute	1.1°×1.1°	ESM	Yukimoto et al. (2012)
NorESM1-M	Norwegian Climate Center	2.5°×1.9°	ESM	Zhang et al. (2012)

ESM Earth System Model, *AOGCM* Atmosphere–Ocean Coupled General Circulation Model

atmosphere, with calculations at the daily and sub-daily time scales, which allows for a better description of the trajectories of atmospheric moisture. In essence, the DRM computes how much moisture is collected from surface evaporation by an atmospheric column, and how much this air column loses via precipitation, while it is advected horizontally by an effective 2D wind field derived from the vertical integral of the horizontal water vapor flux and the total column water vapor. This approach assumes that the water vapor is well mixed in each atmospheric column, such that the ratio of precipitation from local origin (i.e. from surface evaporation within the atmospheric column) to precipitation from advected moisture is equal to the ratio of the column water vapor from local origin to the column water vapor from advected origin.

This assumption can miss important details in the transport of moisture and recycling associated with regions of strong wind shear and/or fast recycling (e.g. Goessling and Reick 2013; Dominguez et al. 2020). However, the 2D version of the DRM used in this study has been able to provide estimates of precipitation recycling and moisture transport over parts of South America that is in agreement with estimates of more complex 3D models (e.g. Martinez and Dominguez 2014; Hoyos et al. 2018; Dominguez et al. 2020). Furthermore, this version of the DRM has been useful for studying contrasts and anomalies related to opposite phases of El Niño-Southern Oscillation (ENSO), droughts, and land-cover changes (e.g. Morales et al. 2020; Roy et al. 2019; Herrera-Estrada et al. 2019; Ruiz-Vásquez et al. 2020). In particular, Morales et al. (2020) show that different 2D versions of the DRM provide the same sign of anomalies and correlations for the transport of atmospheric moisture over the tropical Americas during different ENSO phases. In addition, the 2D DRM is a very simple computational tool that can be used efficiently to compute statistics related to the recycling of moisture and atmospheric moisture transport for multiple models, in contrast to the large computational costs of more comprehensive water vapor transport models (e.g. Dirmeyer et al. 2009; Stohl and James 2004).

The DRM requires data for precipitation, evaporation, precipitable water, and Vertically Integrated Moisture Fluxes (VIMF) at daily time scale. The reference run was performed using input data from the ERA5 reanalysis (Hersbach et al. 2020), at a resolution of 30 km grid size for the period 1980–2005 in the domain between latitudes 20° S–35° N and longitudes 120° W–10° W, as shown in Fig. 1. We considered 11 continental and 8 oceanic regions (Fig. 1). In particular, we focused on the water vapor transport and recycling for three continental regions in tropical South America: Northern South America (NOSA), Northern Amazon (NAMZ) and Southern Amazon (SAMZ).

We also run the DRM using the historical simulations of 11 CMIP5 models (Table 1) during the period 1980–2005
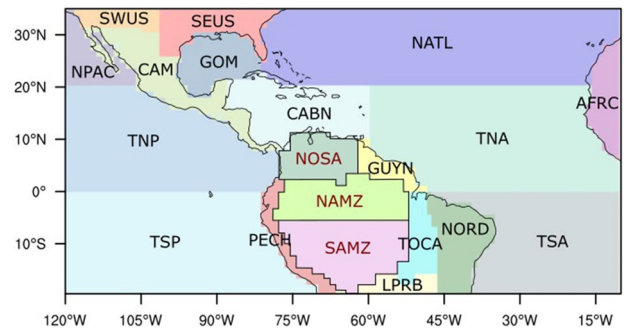

Fig. 1 Domain considered for estimating water vapor transport over tropical South America using the DRM. *NOSA* Northern South America, *NAMZ* Northern Amazon, *SAMZ* Southern Amazon, *TNP* Tropical North Pacific, *TSP* Tropical South Pacific, *NATL* North Atlantic, *TNA* Tropical North Atlantic, *TSA* Tropical South Atlantic, *CABN* Caribbean Sea, *CAM* Central America, *GOM* Gulf of Mexico, *GUYN* Guyanas, *PECH* Peru–Chile, *TOCA* Tocantins basin, *NORD* Brazilian Northeast, *LPRB* La Plata River Basin, *AFRC* Africa, *SWUS* Southwestern United States, *SEUS* Southeastern United States. The delimitation of the regions presented in the figure is based on the horizontal resolution of the MPI-ESM-MR model (1.875° × 1.875°). NOSA, NAMZ, and SAMZ are the sink regions of interest for this study

and their projections under the RCP8.5 scenario for the period 2070–2100. Evaporation, precipitable water and VIMF were computed from the daily CMIP5 outputs for latent heat flux, specific humidity and horizontal wind. The DRM was run with the input data from each CMIP5 model at their original horizontal resolution (Table 1), considering the spatial domain and regions presented in Fig. 1.

2.4 Model evaluation

We used Taylor diagrams (Taylor 2001) to evaluate the ability of the CMIP5 models considered to simulate the variables used by the DRM to estimate atmospheric moisture transport in tropical South America. This method allows evaluating the model performance by comparing the spatial correlation, standard deviation and root mean square error (RMSE) of the model simulation with respect to a reference dataset. Particularly, we evaluated the simulation of precipitation (P), evaporation (E), precipitable water (PW) and P–E by comparing CMIP5 historical simulations against ERA5 estimates during the period 1980–2005. It is important to highlight that although it has been widely discussed that reanalysis products exhibit large biases simulating precipitation (Serreze and Hurst 2000; Rusticucci et al. 2014; Essou et al. 2016; Ceglar et al. 2017), we considered ERA5 as the reference dataset for this variable since DRM requires physically-consistent estimates of P, E and PW; therefore these variables need to come from a physically-consistent product such as a reanalysis and not from independent datasets. Although ERA5 shows suspicious changes in global water

vapor before the early 1990s, they are observed mainly over the tropical oceans (Allan et al. 2022). In general, ERA5 has a broad agreement with satellite records in terms of large-scale precipitation fields (Watters et al. 2021).

To analyze the performance of the CMIP5 models representing the different contributions of PW and P from the different source regions to NOSA, NAMZ and SAMZ (Fig. 1), we compared the mean total annual and mean annual cycles of the contributions estimated with the DRM for each CMIP5 model with those from ERA5. Finally, we estimated the projected changes in the different contributions of PW and P to NOSA, NAMZ and SAMZ by estimating the projected change between the RCP8.5 projection (2070–2100) and the historical simulation (1980–2005) of each CMIP5 model.

3 Results

3.1 Historical simulations of the variables involved in the estimation of atmospheric moisture transport

Different studies have already focused on how the CMIP5 models simulate different hydroclimatic variables in tropical South America, particularly precipitation (Yin et al. 2013; Sierra et al. 2015; Palomino-Lemus et al. 2015, 2017; Arias et al. 2021b; Ortega et al. 2021). Here, we do not attempt to provide a comprehensive assessment of the biases of the CMIP5 models in representing these variables over the region. However, it is important to get a general view of such biases since these variables are required by the DRM to estimate the contributions of PW and P from each moisture source to the sink region of interest (NOSA, NAMZ and SAMZ).

CMIP5 models exhibit their greatest biases simulating mean precipitation in tropical South America during boreal winter and spring (December to February (DJF) and March to May (MAM), respectively (see Figure S1) as previously highlighted in different studies (Yin et al. 2013; Sierra et al. 2015; Ortega et al. 2021), and which is particularly related to a biased ITCZ location (Hirota and Takayabu 2013; Zhang et al. 2015). This ITCZ bias is still observed in the most recent GCM generation (Tian and Dong 2020; Zhou et al. 2020; Ortega et al. 2021). When comparing the simulation of precipitation in continental and oceanic regions, it is clear that the lowest spatial correlations and highest standard deviations are observed for the oceanic regions, mainly in DJF and MAM (Figure S1c). This indicates that the models have more difficulties when simulating this variable over the oceans surrounding tropical South America than over the continental regions. However, an analysis of the annual cycle of precipitation shows that the CMIP5 models underestimate precipitation in NOSA, NAMZ and SAMZ, although they adequately represent the phase of the annual cycle over these regions (not shown). This agrees with previous studies that highlight that the CMIP5 models underestimate precipitation in the Amazon, mainly during its dry season (Joetzjer et al. 2013; Yin et al. 2013; Martins et al. 2015). Among the 11 models considered, the MIROC models show higher spatial correlation coefficients, lower standard deviations and lower RMSE when representing seasonal precipitation in tropical South America, exhibiting a better performance for this variable than the other models. In particular, MIROC5 has been shown to have a reasonable simulation of seasonal precipitation in tropical South America (Palomino-Lemus et al. 2015; Bonilla-Ovallos and Mesa-Sánchez 2017; Sierra et al. 2018; Ortega et al. 2021).

Regarding evaporation, the CMIP5 models considered show their greatest biases over the continental regions than over the oceans (Figure S2). This could be related to the difficulties exhibited by models in representing land-surface interactions, in which soil moisture and land cover play an important role (Koster et al. 2002; Dirmeyer et al. 2013a, b; Lorenz et al. 2016). In particular, they underestimate evaporation over the Amazon mainly during the dry season [June to August (JJA)] and the dry-to-wet transition season [September to November (SON)] (not shown), in agreement with previous studies (Martins et al. 2015). As discussed by Sörensson and Ruscica (2018), there are large uncertainties in the evaporation estimates for South America, particularly over the Amazon, which is observed not only in CMIP models but also in reanalysis and satellite products. When comparing the simulation of this variable by the CMIP5 models considered, MIROC5 is the model with the best metrics according to the Taylor diagrams (Figure S2).

In contrast, CMIP5 models exhibit a much better simulation of precipitable water in comparison to precipitation and evaporation, over both oceanic and continental regions, as suggested by the higher spatial correlation coefficients, lower standard deviations and lower RMSE for this variable (Figure S3). As identified for evaporation, MIROC5 is the model with the best simulation of seasonal precipitable water over tropical South America.

Another variable of interest when analyzing water vapor transport is P–E, which couples the moisture budget between the land and the atmosphere. In the long term, a region with P < E (P–E < 0) denotes a moisture source while regions with P > E (P–E > 0) correspond to moisture sinks. Figure 2 shows that in general, the CMIP5 models considered are able to identify if a particular region is a moisture source or sink during the historical period (1980–2005), as indicated by the high agreement among models simulating this feature for the main oceanic and continental regions presented in Fig. 1. For instance, the oceans behave as moisture sources and the models adequately represent this feature. The seasonal
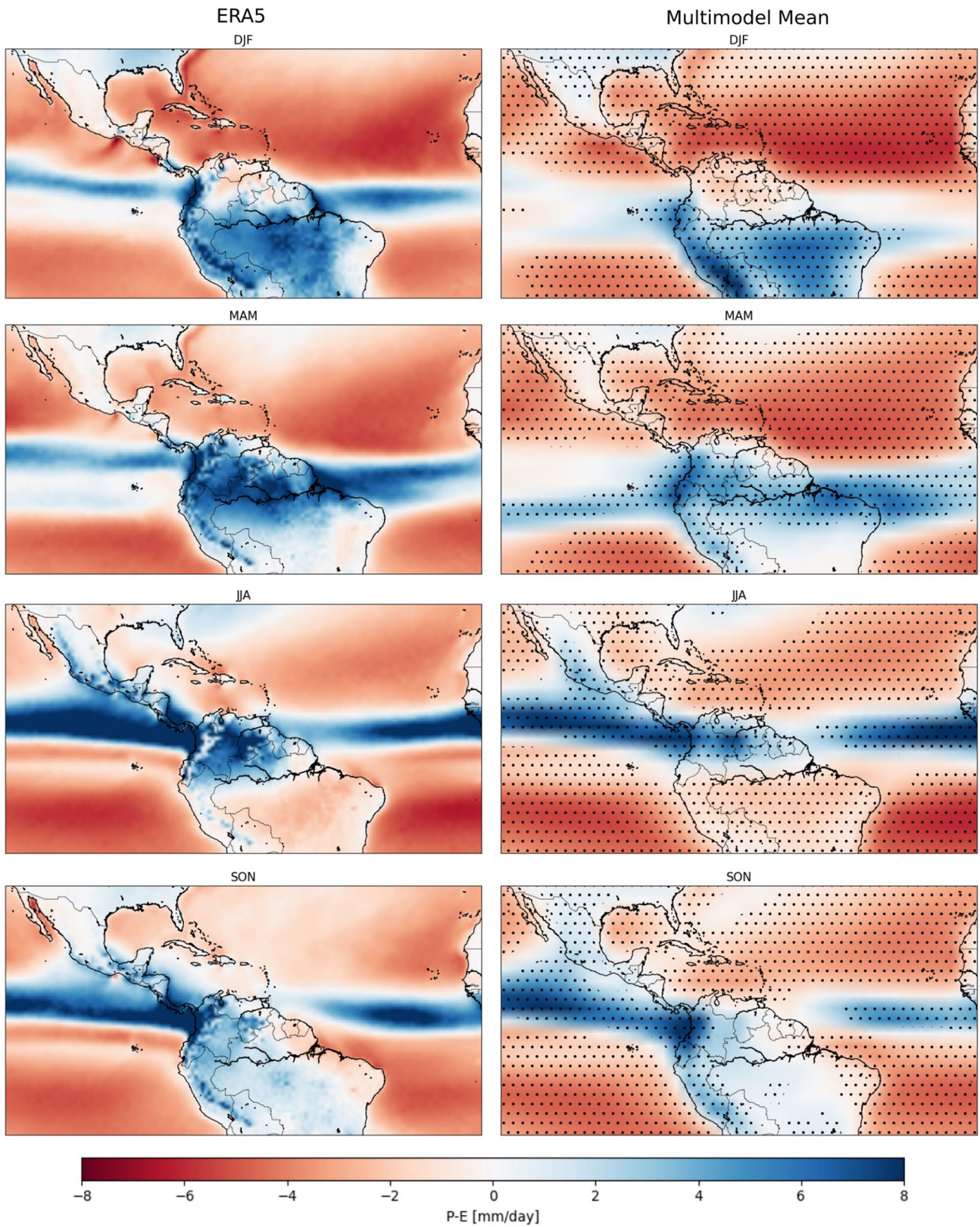
Fig. 2 Multiannual seasonal P–E (in mm/day) over tropical South America simulated by ERA5 (left) and the multimodel mean of the 11 CMIP5 models considered (right) for the period 1980–2005. Red (blue) colors indicate atmospheric moisture sources (sinks). Dots indicate that at least 80% of the models agree on the sign of P–E (i.e. they agree on whether there is a moisture source or a moisture sink)

meridional migration of the ITCZ, evidenced by P–E > 0 over the tropical oceans, is simulated by most of the models, indicating the occurrence of moisture convergence over the region. In contrast, most of the continental regions behave as moisture sinks. However, the southern Amazon acts as a moisture source mainly during its dry season (JJA), which is correctly represented by the models, except CanESM2 (Figure S5l).

P–E is better simulated by the models over the continent during DJF and MAM while the oceanic patterns are better represented during JJA and SON (Figure S4). The greatest biases of P–E over the oceanic regions during DJF and MAM (Figure S4c) agree with the seasonal biases of precipitation over these regions (Figure S1c). Also, the largest biases over the continent in JJA and SON (Figure S4b) agree with the greatest biases of evaporation over these regions (Figure S2b). This suggests that the simulation of P–E in tropical South America by the CMIP5 models is strongly biased by their simulation of precipitation over the oceans and evaporation over the continental regions. Among the CMIP5 models, the MIROC models exhibit the best simulation of the P–E seasonal spatial patterns while the MRI models exhibit the poorest simulation, according to the Taylor diagrams (Figure S4).

To understand the origin of these biases is beyond the scope of this work as it involves investigating each of the land-surface schemes of the input models, along with each of the components related to hydrological variables in those models. Evaporation biases can also be a result of precipitation and circulation biases (e.g. if the region is unrealistically dry in terms of precipitation then there will also not be enough soil water to evaporate) in addition to the physical models employed to represent bare soil and vegetated evaporation and transpiration.

3.2 Historical simulations of atmospheric moisture transport

We used the DRM, with inputs from ERA5 and different CMIP5 models (Table 1), to estimate the contributions to PW and P from different regions to NOSA, NAMZ and SAMZ (see Fig. 1). The DRM estimates from ERA5 inputs are used as the reference (reference run). We run the DRM using input data at the original horizontal resolution of each CMIP5 model and compared with the ERA5 reference run. In general, CMIP5 models are able to capture the main atmospheric moisture sources to NOSA, NAMZ and SAMZ as observed from the ERA5 reference run (Figs. 3, 4, 5).

For NOSA (Fig. 3), the main sources for both PW and P are the Tropical North Atlantic (TNA), NOSA (i.e. moisture recycling), the Tropical South Atlantic (TSA) and the North Atlantic (NATL). Although it is not a dominant source throughout the year, NAMZ provides significant moisture to

NOSA in JJA (Figure S6). These sources have been previously identified (Sakamoto et al. 2011; Poveda et al. 2014; Arias et al. 2015b; Hoyos et al. 2018). For NAMZ (Fig. 4), the main moisture sources are TNA, TSA, NAMZ (i.e. moisture recycling) and the Brazilian Northeast (NORD). In particular, the contribution of the Atlantic sources to atmospheric moisture in NAMZ has been previously documented (Bosilovich and Chern 2006; Drumond et al. 2008, 2014; Satyamurty et al. 2013; Rocha et al. 2017; Sori et al. 2018; Agudelo et al. 2019). Finally, the main sources of atmospheric moisture for SAMZ (Fig. 5) are SAMZ itself (moisture recycling), TSA, TNA, NAMZ and NORD. The relevant role of atmospheric moisture recycling over SAMZ (reaching values about 20–30% according to our DRM estimates) has been widely discussed (e.g. Zemp et al. 2014; Swann et al. 2015; Marengo et al. 2017; Rocha et al. 2017; Staal et al. 2018; Ampuero et al. 2020; Ruiz-Vásquez et al. 2020; Tuinenburg et al. 2020; Dominguez et al. 2022).

When analyzing the annual cycle of the atmospheric moisture contributions from the different source regions to NOSA, NAMZ and SAMZ (Figures S6 to S8), the largest biases exhibited by the CMIP5 models (with respect to the ERA5 reference run) correspond to their simulations of PW and P recycling over these three continental regions, while they have a better representation of the atmospheric moisture transport from the oceans. This could be related with the strong biases shown by the models simulating evaporation over the continental regions of tropical South America (Figure S2c). Also, the correlations between the simulated annual cycle of transported moisture and that from ERA5 are lower when considering atmospheric moisture transport from the continental regions toward the Amazon (NAMZ and SAMZ) in comparison with the transport from the oceanic regions, particularly for PW (Figures S7 and S8).

Table 2 shows the models with the best representation of the annual cycle of PW and P transported from the main moisture sources to NOSA, NAMZ and SAMZ. In general, MIROC5 is the model with the best representation of atmospheric moisture transport and recycling for the three sink regions considered. This could be related to the fact that MIROC5 is also one of the best models for simulating P, E, PW and P–E (Figures S1 to S4).

3.3 Projections of the variables involved in the estimation of atmospheric moisture transport

In order to identify the main projected changes in P, E, PW and P–E that may affect future PW and P transport over tropical South America, we present a brief summary of these projections based on the 11 CMIP5 models considered for the different regions shown in Fig. 1. This summary is presented in Fig. 6.
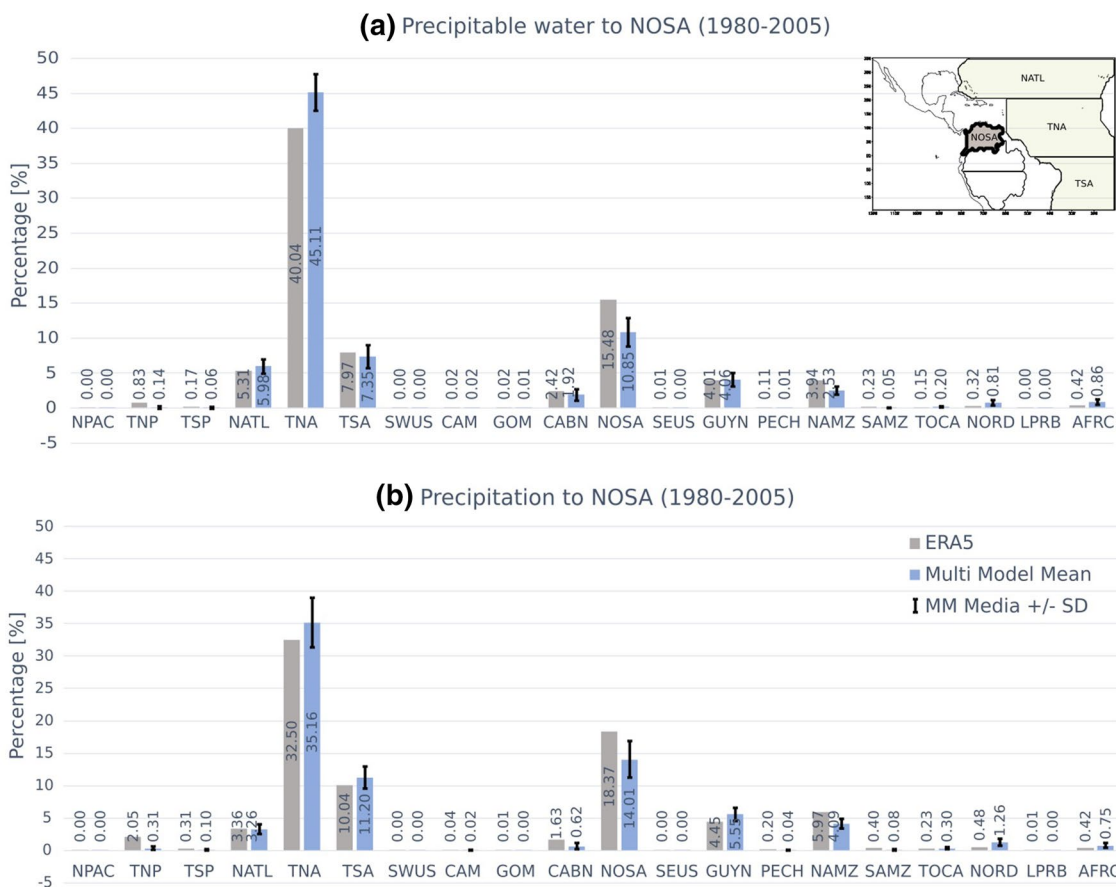
Fig. 3 Total annual contributions (in %) to **a** precipitable water and **b** precipitation from each of the source regions presented in Fig. 1 to NOSA during the period 1980–2005. The grey bar indicates ERA5 estimates and blue bars show the mean of the 11 models considered. The whiskers show the standard deviation among the 11 CMIP5 models. The inset map shows the sink region (grey shades) and the main source regions (blue shades)

Projections indicate an increase of precipitable water over all the regions considered in tropical South America, with 100% of agreement among models for all the seasons, while evaporation is projected to increase mainly over the oceans. In general, oceanic regions are projected to become stronger moisture sources by the end of the twenty-first century. However, precipitation changes are spatially heterogeneous. Precipitation is projected to increase over the continental regions during DJF. In contrast, decreases of precipitation are projected over SAMZ by the end of the twenty-first century during JJA and SON, with reductions of about 32% and 19%, respectively, with respect to the historical period.

For the continental regions of interest in this study, precipitation is projected to reduce over NOSA for DJF and JJA, with high agreement between models (81.8%). Likewise, projections suggest reductions of precipitation in NAMZ during JJA and SON, with strong model agreement (100% and 90.9%, respectively). Over SAMZ, models agree in a reduction of precipitation during these

seasons (90.9% of agreement) while evaporation is projected to decrease, although with less agreement between models (72.7% and 81.8%, respectively).

Regarding P–E, the CMIP5 models analyzed agree on a projected strengthening of the oceans as a moisture source by the end of the twenty-first century, although the projected change exhibits different magnitudes among the ocean regions considered. The only exception is the Tropical North Pacific (TNP), which is projected to intensify its role as a moisture sink by the late twenty-first century. To understand this difference is beyond the scope of our current study, which focused on recycling over the landmass of tropical South America. In contrast, projections of P–E over the continental regions exhibit lower agreement. However, it is interesting to note that the models generally agree on a weakening of NOSA (during JJA and SON), NAMZ (during SON) and SAMZ (SON) as moisture sinks, with a model agreement of 90.9%, 75% and 81.8%, respectively.
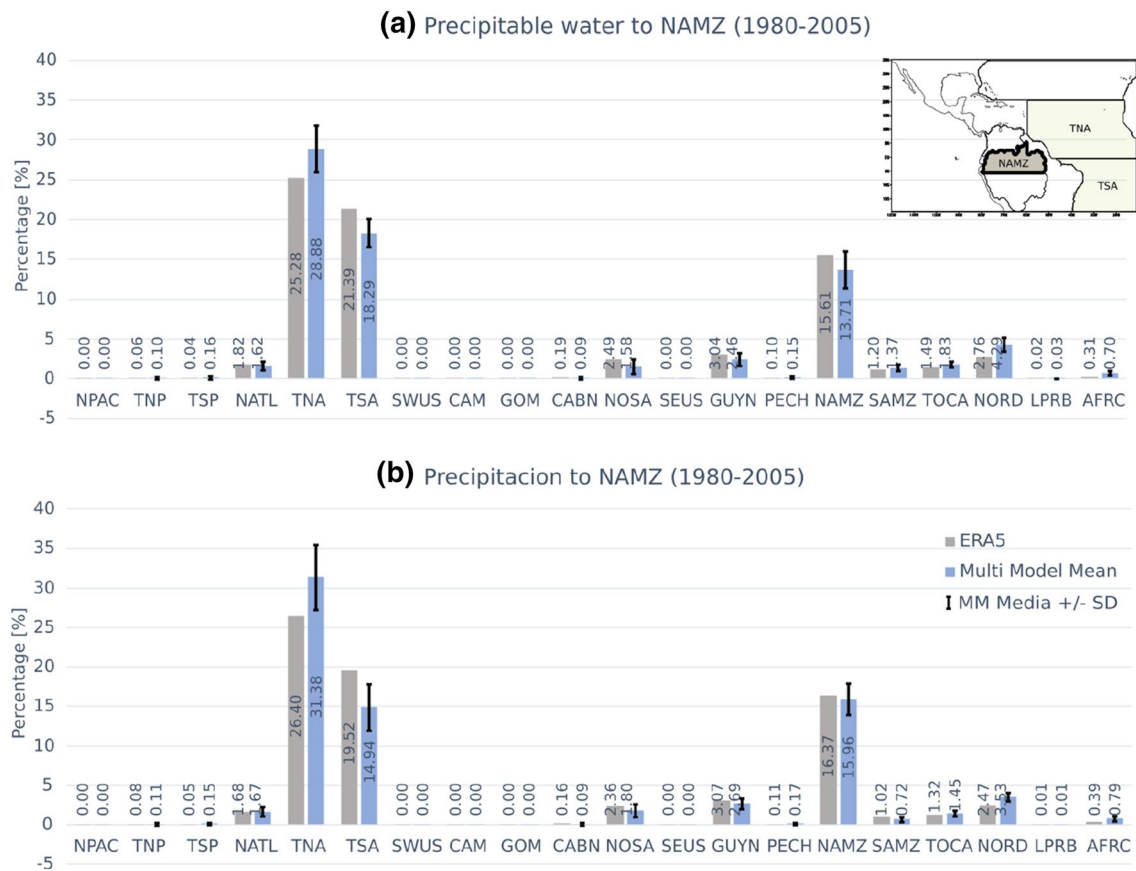
Fig. 4 Total annual contributions (in %) to **a** precipitable water and **b** precipitation from each of the source regions presented in Fig. 1 to NAMZ during the period 1980–2005. The grey bar indicates ERA5 estimates and blue bars show the mean of the 11 models considered. The whiskers show the standard deviation among the 11 CMIP5 models. The inset map shows the sink region (grey shades) and the main source regions

3.4 Projections of atmospheric moisture transport

Climate change induced by increasing GHG concentrations is expected to intensify but modify the regional characteristics of atmospheric moisture transport (Lavers et al. 2015; Zhang et al. 2021; Yang et al. 2022). Therefore we analyzed the projected changes in the transport and recycling of atmospheric moisture contributing to PW and P over the three continental regions of interest in tropical South America by the late twenty-first century under the RCP8.5 scenario. We estimated the projected change for each source region as the difference between the mean transport under the RCP8.5 projection (2070–2100) and the mean transport from the historical simulation (1980–2005) for each CMIP5 model considered. Changes are expressed as a percentage with respect to the historical mean. Figures 7, 8, 9 show the projected changes in the transport from the main source regions contributing to PW and P over NOSA, NAMZ and SAMZ, respectively, according to the 11 models considered.

For NOSA (Fig. 7), there is a high model agreement on the projected increases of atmospheric moisture contributions from the Atlantic sources (TNA, TSA and NATL) during the year, with higher agreement for the northern Atlantic regions. Also, models generally agree on a projected increase of PW recycling over NOSA throughout the year (agreement about 70%; Fig. 7a). The total PW is projected to increase over NOSA by the end of the twenty-first century in about 30% with respect to the historical period, with high model agreement (Fig. 7a). Projections suggest that contributions from TNA, NOSA and NAMZ will represent a smaller fraction of the total PW by the end of this century (Fig. 7b). The negative values in Fig. 7b indicate that the relative contribution of water vapor from these regions to NOSA will be smaller under the RCP8.5 scenario than under historical conditions. This means that the fraction of PW transported from these sources to NOSA with respect to the total PW in NOSA will be reduced by the end of the twenty-first century, which is suggested by most of the CMIP5 models considered. By contrast, the relative PW contributions from TSA and NATL in MAM are projected to increase (Fig. 7b), indicating that the fraction of PW transported from these regions will increase in the future
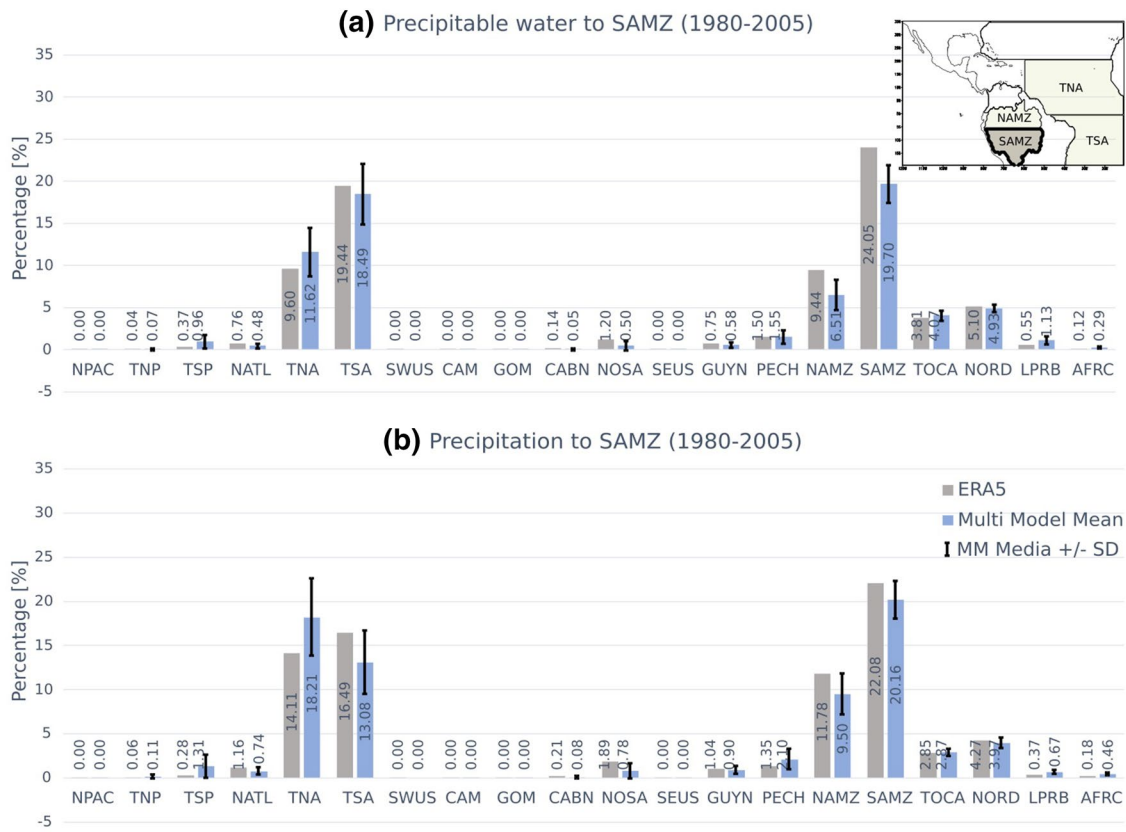
(a) Precipitable water to SAMZ (1980-2005)

(b) Precipitation to SAMZ (1980-2005)

■ ERA5
■ Multi Model Mean
I MM Media +/- SD

Fig. 5 Total annual contributions (in %) to **a** precipitable water and **b** precipitation from each of the source regions presented in Fig. 1 to SAMZ during the period 1980–2005. The grey bar indicates ERA5 estimates and blue bars show the mean of the 11 models considered. The whiskers show the standard deviation among the 11 CMIP5 models. The inset map shows the sink region (grey shades) and the main source regions

Table 2 Models with the best performance simulating seasonal transport of PW and P from the main source regions to NOSA, NAMZ and SAMZ, with respect to ERA5

		Correlations with ERA5			
Sink region	Source region	Transported PW		Transported P	
NOSA	**TNA**	CanESM2	0.97	MPI-ESM-MR	0.93
	NOSA	MIROC5	0.92	MIROC5	0.94
	TSA	CanESM2	0.99	CanESM2	0.99
	NATL	MPI-ESM-MR	0.98	MPI-ESM-MR	0.85
	NAMZ	MRI-ESM1	0.93	MIROC-ESM-CHEM	0.98
NAMZ	**TNA**	CanESM2	0.99	CanESM2	0.97
	TSA	CanESM2	0.99	CanESM2	0.96
	NAMZ	MRI-ESM1	0.92	MIROC5	0.95
	NORD	MIROC5	0.99	MIROC5	0.95
	SAMZ	MIROC-ESM-CHEM	0.94	MIROC-ESM-CHEM	0.87
SAMZ	**SAMZ**	MRI-CGCM3	0.94	MRI-ESM1	0.99
	TSA	MRI-ESM1	0.90	MIROC5	0.93
	TNA	MPI-ESM-MR	0.99	MPI-ESM-MR	1.00
	NAMZ	MIROC5	0.98	MIROC5	0.99
	NORD	MPI-ESM-MR	0.87	MPI-ESM-MR	0.93

Numbers indicate the correlation coefficient between the simulated annual cycle and that of ERA5. Dark shades indicate the models with the largest correlation with ERA5
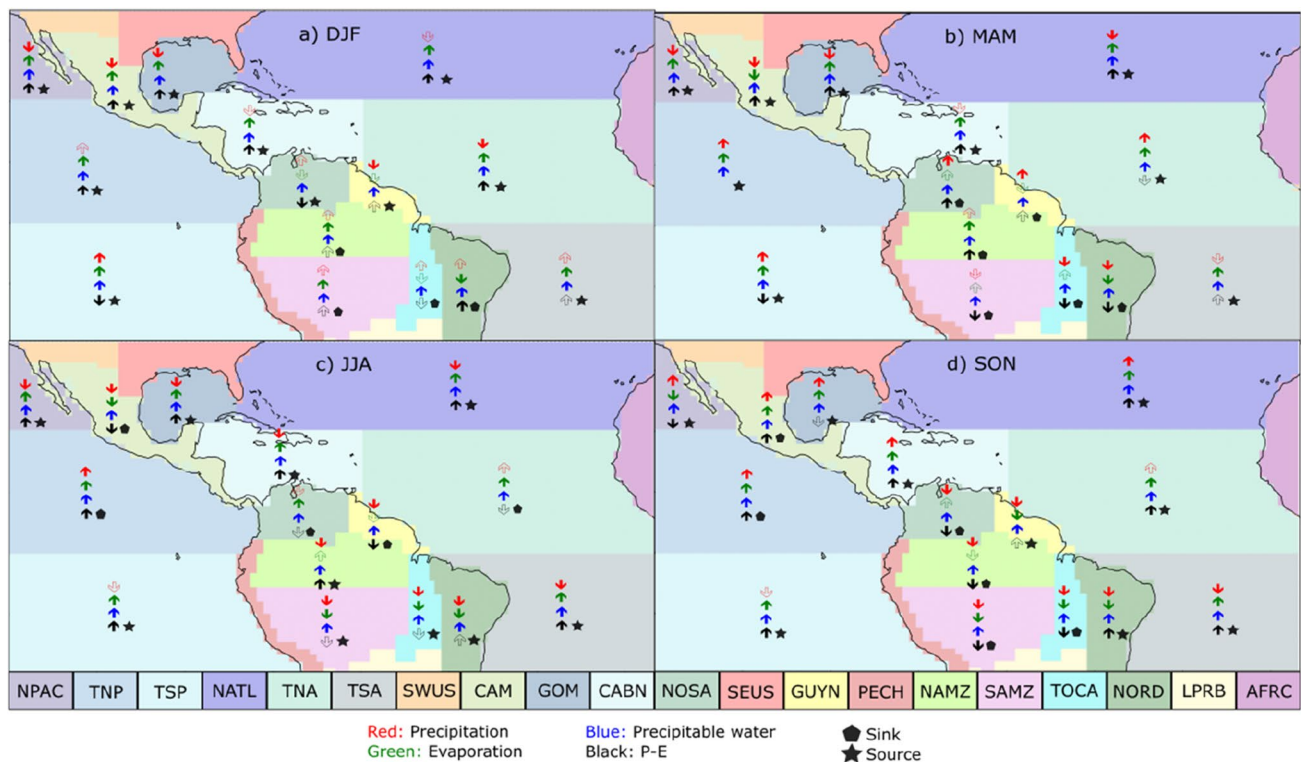
Fig. 6 Sign of projected change by the end of the twenty-first century (2070–2100) under the RCP8.5 scenario for the four variables considered: precipitation (red), evaporation (green), precipitable water (blue) and P–E (black). Bold (empty) arrows indicate that at least (less than) 70% of the models agree on the sign of the projected change. The consensus is estimated for the different regions presented under the RCP8.5 scenario. Regarding the contributions to P over NOSA, projections suggest lower model agreement and more mixed signals (Fig. 7c). For instance, contributions to P from TNA are projected to increase during DJF and MAM and to decrease in JJA and SON, although model agreement is below 70%. Projected changes of total P over NOSA indicate increases during DJF and MAM, and decreases during JJA and SON. Increases of total P during DJF and MAM are related to the increases in moisture transport from the Atlantic source regions (TNA, TSA and NATL), while the reductions of total P during JJA and SON are related to the reduced contributions from both oceanic and continental sources. NAMZ is the region with the greatest projected reduction in its contribution to P over NOSA (about 35–36%). Reductions in the transport from continental sources (NOSA and NAMZ) are also observed during JJA and SON and 100% of models agree on a projected reduction of the relative contribution to the P from local recycling over NOSA. The projections analyzed here suggest that, although the column water vapor from local origin (i.e. recycled PW) is projected to increase over NOSA, this is not reflected in an increase in recycled P. By contrast, recycled P in Fig. 1. Upward (downward) arrows indicate a projected increase (decrease) of the variable. The star symbol indicates that the region is projected to behave as a moisture source (P < E). The pentagon symbol indicates that the region is projected to behave as a moisture sink (P > E). The panels correspond to a particular season: **a** DJF, **b** MAM, **c** JJA, and **d** SON

over NOSA is projected to decrease by the end of the twenty-first century under the RCP8.5 scenario, with a higher model agreement for JJA and SON (81.1% and 100% of agreement, respectively). This means that although the recycled PW over NOSA is projected to increase, the recycled P over the region is projected to reduce such that locally evaporated moisture is more readily retained in the atmosphere rather than leading to precipitation.

For NAMZ (Fig. 8), models exhibit a high agreement on projected increases of PW transported from its main moisture sources, in particular TNA and TSA. Likewise, there is high agreement on projected increases of PW recycling over NAMZ during DJF and MAM. Total PW over NAMZ is projected to increase in about 25% of models with respect to the historical period. Projections also indicate that the PW contributions from TNA, NAMZ, NORD and SAMZ will represent a smaller fraction of the total PW in NAMZ (Fig. 8d). By contrast, PW contributions from TSA are projected to represent a larger fraction of the total PW by the end of the twenty-first century, mainly during DJF, MAM and SON. Regarding contributions to P (Fig. 8c), projections exhibit lower model agreement. However,
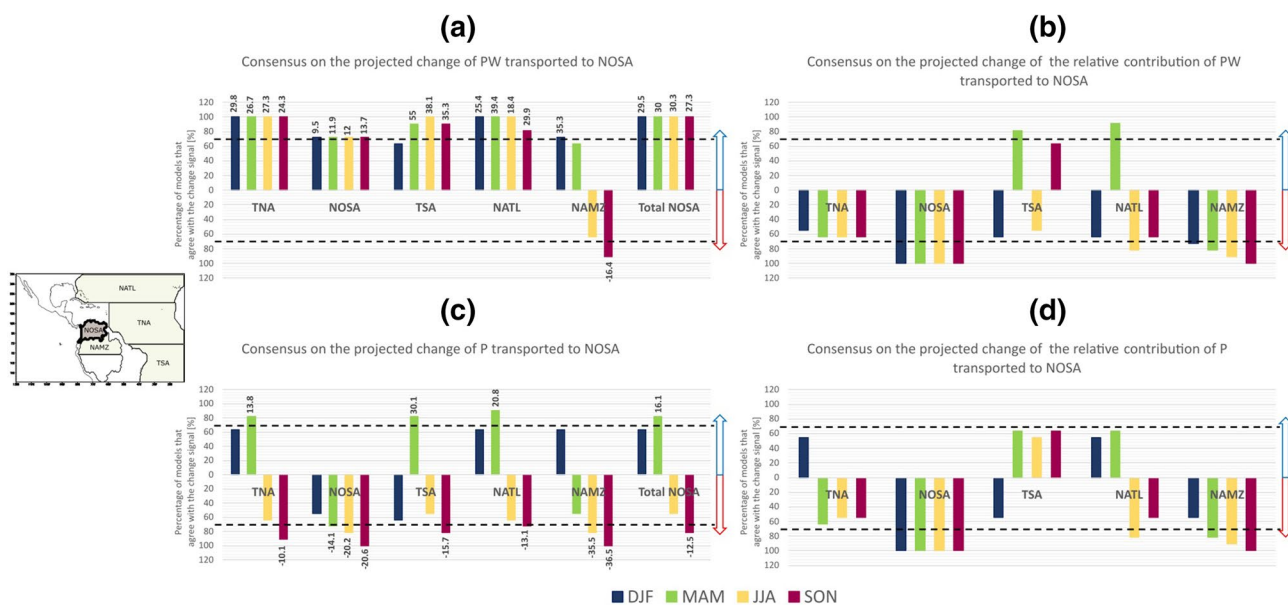
Fig. 7 Consensus among the 11 CMIP5 models considered on the projected change of atmospheric moisture transport toward NOSA by the end of the twenty-first century. **a** Consensus (in %) on the projected change of PW transported from the main source regions to NOSA. **b** Consensus (in %) on the projected change of the relative contribution of PW transported from the main source regions with respect to the total PW in NOSA. **c** As in **a** but for P. **d** as in **b** but for P. Source regions are presented in decreasing order of contribution of atmospheric moisture to NOSA in the historical period (1980–2005). Colors indicate the different seasons of the year: DJF (blue), MAM (green), JJA (yellow), and SON (red). Dashed lines indicate

a 70% of agreement between models. Numbers accompanying each bar in **a**, **c** indicate the mean percent change of the projected transport (2070–2100) with respect to the historical period (1980–2005) for those models with agreement in the sign of the projected change. Bars that do not include this number correspond to estimates with low agreement between models (less than 70%). In **a**, **c**, Total NOSA indicates the consensus on the projected change of the total PW and total P, respectively, over NOSA by the end of the twenty-first century (2070–2100). The inset map shows the sink region (grey shades) and the main source regions

there is high agreement on projected reductions in contributions to P over NAMZ from TNA during MAM, JJA and SON. P recycling over NAMZ is projected to decrease during most of the seasons with 100% of model agreement during JJA and SON. Total P over NAMZ is projected to increase during DJF in association with increased contributions to P from TSA (DJF and MAM), NORD (DJF) and SAMZ (DJF) (Fig. 8c). By contrast, total P in NAMZ is projected to decrease during JJA and SON due to the reductions in the contributions to P from its main moisture sources. In particular, our results suggest that two of the three main continental moisture sources for NAMZ (i.e. NORD and SAMZ) will decrease their contributions to P during JJA and SON, reaching up to a reduction of 51% with respect to the historical relative contribution during SON. As observed for NOSA, although the recycled PW over NAMZ is projected to increase (Fig. 8a), the recycled P over the region is projected to decrease (Fig. 8c). In fact, the relative contribution to the recycling of P over NAMZ is projected to decrease by the end of the twenty-first century (Fig. 8d). TSA is the only moisture source region that is projected to increase its relative contribution of P to NAMZ for all the seasons, except SON (Fig. 8d).

Similar to NOSA and NAMZ, the PW contributions from the main oceanic source regions to SAMZ (TNA and TSA) are projected to increase in magnitude (Fig. 9a). Also, PW contributions from SAMZ (during DJF and MAM), NAMZ (during DJF and JJA) and NORD (during DJF and MAM) are projected to increase with model agreement higher than 70%. The total PW over SAMZ is projected to increase by the end of the twenty-first century, with increases between 20 and 28% with respect to the historical period (Fig. 9a, right column). These increases are mainly related to increased PW transported from TSA, whose PW contributions are projected to represent a larger fraction of the total PW in SAMZ by the end of the century (Fig. 9b). The relative importance of the PW contributions from TNA and NORD to SAMZ is also projected to increase. By contrast, the relative importance of the PW contributions (i.e. fractional contributions) from SAMZ (i.e. PW recycling) is projected to decrease (Fig. 9b). Regarding contributions to P, projections suggest a reduction of P recycling over SAMZ during all the seasons by the end of the twenty-first century, with greater reductions in JJA (40%) and SON (31%) (Fig. 9c). Also, there is high agreement on
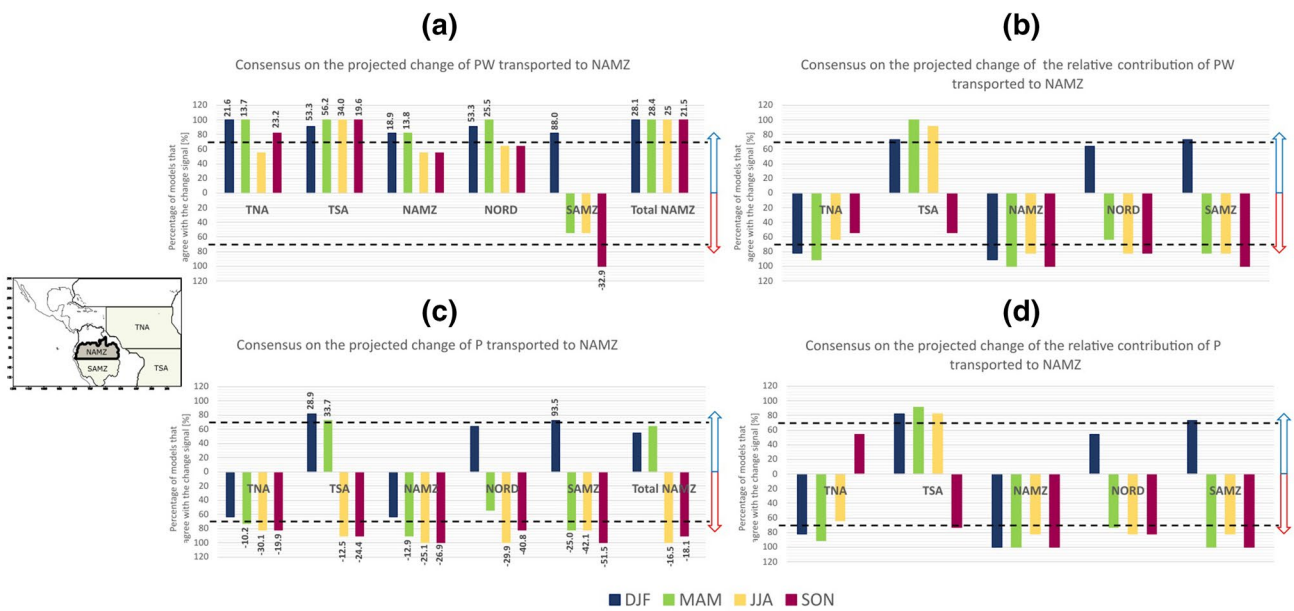
Fig. 8 Consensus among the 11 CMIP5 models considered on the projected change of atmospheric moisture transport toward NAMZ by the end of the twenty-first century. **a** Consensus (in %) on the projected change of PW transported from the main source regions to NAMZ. **b** Consensus (in %) on the projected change of the relative contribution of PW transported from the main source regions with respect to the total PW in NAMZ. **c** As in **a** but for P. **d** As in **b** but for P. Source regions are presented in decreasing order of contribution of atmospheric moisture to NAMZ in the historical period (1980–2005). Colors indicate the different seasons of the year: DJF (blue), MAM (green), JJA (yellow), and SON (red). Dashed lines indicate a 70% of agreement between models. Numbers accompanying each bar in **a**, **c** indicate the mean percent change of the projected transport (2070–2100) with respect to the historical period (1980–2005) for those models with agreement in the sign of the projected change. In **a**, **c**, Total NAMZ indicates the consensus on the projected change of the total PW and total P, respectively, over NAMZ by the end of the twenty-first century (2070–2100). The inset map shows the sink region (grey shades) and the main source regions

the reductions in the contributions to P from TSA during JJA and SON, TNA and NAMZ during the entire year, and NORD during MAM, JJA and SON (Fig. 9c). P total over SAMZ is projected to increase in magnitude during DJF and decrease during MAM, JJA and SON. The P total increases during DJF seem to be related to the projected increases in the contributions to P from TSA and NORD. The P total decreases during MAM, JJA and SON are consistent with the reductions of contributions to P from the main moisture sources for SAMZ (Fig. 9c). Although these decreases of P contributions are observed for all the main moisture sources, the reduction of P contributions from the continental sources is remarkable since they exhibit the largest reductions in terms of their relative contribution to total P over SAMZ. For instance, the relative importance of P recycling over SAMZ is projected to decrease by 40% and 31% during JJA and SON, respectively, while contributions from NAMZ decrease by 41% and 30%, and contributions from NORD decrease by 41% and 32% (Fig. 9d). As also observed for NAMZ, the only moisture source that is projected to increase its relative contribution to total P over SAMZ is TSA.

4 Summary and discussion

This work analyzes the simulation and projections of atmospheric moisture transport influencing tropical South America. We used the Dynamic Recycling Model (DRM) to estimate the contribution of moisture sources to the precipitable water and precipitation across three continental sink regions: Northern South America (NOSA), Northern Amazon (NAMZ) and Southern Amazon (SAMZ) (Fig. 1).

The ability of the CMIP5 models considered in simulating the input variables for the DRM over tropical South America was evaluated. In general, models are able to capture the main seasonal cycle of precipitation (P) over the region, although they exhibit the well-known biased location of the Intertropical Convergence Zone, mainly during boreal winter and spring, as identified in numerous studies (Hirota and Takayabu 2013; Yin et al. 2013; Sierra et al. 2015; Zhang et al. 2015; Ortega et al. 2021). Consistently, the largest biases of simulated P are located over the oceans surrounding tropical South America. For evaporation (E), models exhibit their largest biases over the
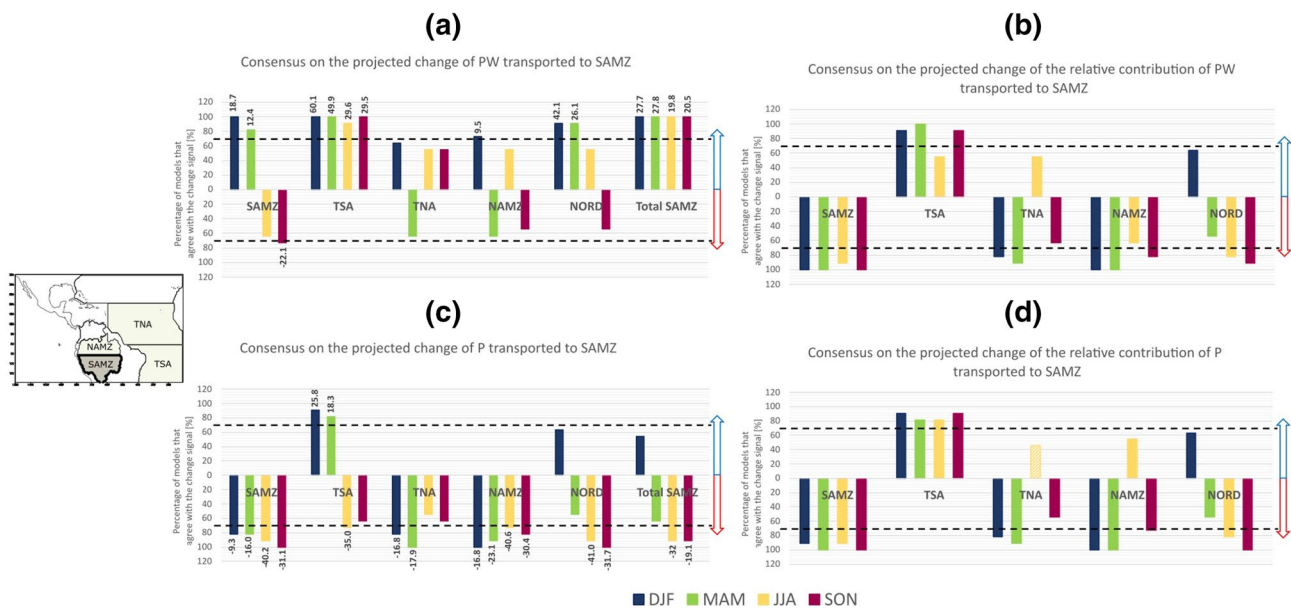
Fig. 9 Consensus among the 11 CMIP5 models considered on the projected change of atmospheric moisture transport toward SAMZ by the end of the twenty-first century. **a** Consensus (in %) on the projected change of PW transported from the main source regions to SAMZ. **b** Consensus (in %) on the projected change of the relative contribution of PW transported from the main source regions with respect to the total PW in SAMZ. **c** As in **a** but for P. **d** As in **b** but for P. Source regions are presented in decreasing order of contribution of atmospheric moisture to SAMZ in the historical period (1980–2005). Colors indicate the different seasons of the year: DJF (blue), MAM (green), JJA (yellow), and SON (red). Dashed lines indicate a 70% of agreement between models. Numbers accompanying each bar in **a**, **c** indicate the mean percent change of the projected transport (2070–2100) with respect to the historical period (1980–2005) for those models with agreement in the sign of the projected change. Bars that do not include this number correspond to estimates with low agreement between models (less than 70%). In **a**, **c**, Total SAMZ indicates the consensus on the projected change of the total PW and total P, respectively, over SAMZ by the end of the twenty-first century (2070–2100). The inset map shows the sink region (grey shades) and the main source regions

continental regions, which could be related to the difficulties exhibited by the models in representing land-surface interactions (Koster et al. 2002; Dirmeyer et al. 2013a, b; Lorenz et al. 2016). The simulation of precipitable water (PW) is much closer to the ERA5 estimates for both oceanic and continental regions than for P and E, indicating that the CMIP5 models considered have a better performance simulating this variable. Finally, the simulation of P–E is mainly affected by the P biases over the oceans and the E biases over the continental regions. Despite these biases, the studied CMIP5 models are able to identify the regions that behave as moisture sources (P–E < 0) and moisture sinks (P–E > 0) over tropical South America during the different seasons (Fig. 2). Among the models considered in this study, the MIROC models exhibit the best performance simulating these variables over tropical South America, particularly MIROC5, according to the analysis of Taylor diagrams (Figures S1 to S4).

Regarding the simulation of the transport of atmospheric moisture, and its contributions to PW and P over the continental regions, our results show that the models considered are in general able to identify the main moisture sources (i.e. their relative importance) for each region. In particular, the

MIROC5 model exhibits the greatest agreement with the ERA5 estimates (Table 2 and Figures S6 to S8). However, when evaluating the annual cycles of PW and P contributions simulated by the models, we identified larger biases for moisture recycling and transport from the continental regions, particularly for the Amazon (NAMZ and SAMZ), than for the atmospheric moisture transported from oceanic regions. Although the CMIP5 models exhibit biases representing P (mainly over the oceans) and E (mainly over the continent) in tropical South America, they capture the observed behavior of atmospheric moisture transport over the region (Figs. 3, 4, 5), which may be a more reliable feature in these models.

We analyzed the projections of the input variables to the DRM under the Representative Concentration Pathway (RCP)-8.5 scenario by the end twenty-first century (Fig. 6). The projections of P are spatially heterogeneous over tropical South America. Our results suggest increased P during December to February (DJF) over most of the regions considered. However, we identified reductions of P over SAMZ during June to August (JJA; dry season) and September to November (SON; dry-to-wet transition season). For the Amazon, this means intensification of the

Fig. 10 Synthesis of the changes of P transport to **a** NOSA, **b** NAMZ and **c** SAMZ projected by the end of the twenty-first century (2070–2100). The scheme shows the seasons and moisture sources with more than 80% of agreement among the 11 CMIP5 models considered. The numbers above the arrows indicate the projected change of P transported (in %) from each moisture source to the respective sink region (only shown for more than 80% of model agreement). Red arrows indicate decreases in the P transported from a particular moisture source. The numbers within the dark circles indicate the order of P contribution from each particular moisture source (1: most contribution, 6: least contribution). The +(−) symbol indicates that the respective moisture source is projected to have a larger (smaller) relative contribution by the end of the twenty-first century. The cloud symbol indicates the projected percent change of total P over the respective sink region. The red recycling symbol indicates projected reductions in recycled P over the sink region. The bold number below the recycling symbol indicates the projected percent change of P recycling. The different values presented in this scheme were estimated based only in the models that agree in the sign of the projected change for each respective moisture source

wet and dry seasons and a drying of the dry-to-wet transition season, which is in agreement with previous studies analyzing CMIP5 (Fu et al. 2013; Boisier et al. 2015; Palomino-Lemus et al. 2017) and CMIP6 projections (Wainwright et al. 2021). Reductions of E over SAMZ are also projected during these seasons. In addition, our analysis suggests projected increases of E over the oceans that are in agreement with previous literature (Levang and Schmitt 2015). This projected increase of oceanic E is related to the increased PW with a warmer climate as suggested by regional (Lavers et al. 2013; Warner et al. 2015) and global studies (Laîné et al. 2014; Lavers et al. 2015). Consistently, oceans surrounding tropical South America are projected to strengthen their role as moisture sources (P–E < 0) with a warmer atmosphere, as suggested by other studies analyzing the global tropics (Liu and Allan 2013).

Finally, we estimated the projected changes of atmospheric moisture transport over tropical South America by the end of the twenty-first century under the RCP8.5 scenario. In general, PW transported from the oceans (mainly the Atlantic regions) to NOSA, NAMZ and SAMZ is projected to increase (Figs. 7, 8, 9). This is consistent with the projected increase of E and PW over the oceanic regions surrounding tropical South America (Fig. 3). Laîné et al. (2014) indicate that the projected increases of atmospheric moisture over the oceans is directly related to the atmospheric warming effect (Clausius-Clapeyron relation) while over the continental regions, the changes in atmospheric water vapor are not necessarily related to the changes of E since they are more related to soil moisture availability over these regions. Particularly, over more arid regions, the moisture source is the ocean and thus changes in land–ocean warming contrast play a role since the lesser ocean warming means that moisture transport cannot keep pace with atmospheric demand and therefore humidity
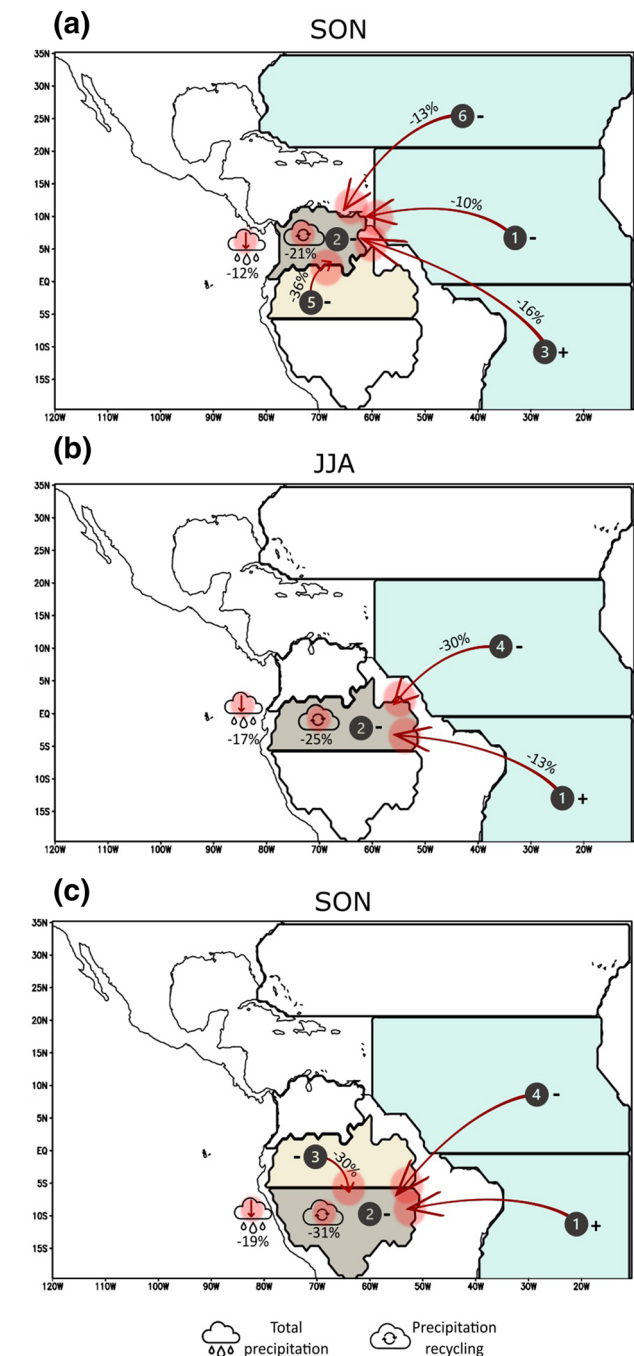
declines (Byrne and O'Gorman 2018; Wainwright et al. 2022).

Figure 10 shows a synthesis of the main projected changes in the contribution of atmospheric moisture transport to precipitation over NOSA, NAMZ and SAMZ during the season with the greatest changes for each region. In general, the three continental regions exhibit similar projected changes: (1) reductions in the contributions to P from their main atmospheric moisture sources, (2) reductions of total P, and (3) reductions of recycled P over the region. For NOSA

(Fig. 10a), our results suggest reductions in contributions to P from TNA, NOSA (recycling), TSA, NAMZ and NATL mainly during SON. Over NAMZ (Fig. 10b), projections show reduced contributions from TSA, NAMZ (recycling) and TNA mainly during JJA. Over SAMZ (Fig. 10c), there is high agreement on projected reductions of contributions from TSA, SAMZ (recycling), NAMZ and TSA mainly during SON. The largest reductions of P recycling (about 31%) are projected over SAMZ during SON, which corresponds to the transition season between dry and wet regimes, followed by NAMZ, which exhibits the largest reductions (about 25%) during its dry season (JJA). The high model consensus on P recycling reductions over SAMZ is consistent with the high agreement exhibited by models on projected reductions of E over this region during JJA and SON (Fig. 3). Despite the general reduction in P, note that (1) there is an increase in the transport of PW, and (2) the changes in the contributions from the different sources are not homogeneous (Figs. 7, 8, 9), rather depending on local fluxes like E as well as on the regional circulation. This suggests that moisture transport can change because of thermodynamic factors (there is more moisture above a warmer ocean) but also dynamic (there is a spatial shift in the wind fields so altering the position of the strongest moisture transport pathways or alternatively there is a strengthening or weakening of the wind fields).

The Amazon has been widely recognized as a climate change hotspot (e.g. Torres and Marengo 2014; Artaxo et al. 2021). According to our results, P recycling, an important moisture source for tropical South America, is projected to decrease by the late twenty-first century, particularly over the Amazon during the dry (JJA) and dry-to-wet transition (SON) seasons. These projections are consistent with other studies analyzing recent climate trends over this tropical river basin. Previous studies have shown the occurrence of longer dry seasons over the southern Amazon during the recent decades (Fu et al. 2013; Arias et al. 2015a; Debortoli et al. 2015; Espinoza et al. 2019; Haghtalab et al. 2020; Giraldez et al. 2020; Correa et al. 2021; Cintra et al. 2022; Xu et al. 2022; Wainwright et al. 2022). In fact, the Sixth Assessment Report (AR6) of the Intergovernmental Panel on Climate Change indicates high confidence on a delayed onset of the South American monsoon during since the late 1970s (Douville et al. 2021), which is related to a longer dry season over the southern Amazon. This lengthening of the southern Amazon dry season is associated with an increased frequency of dry days during the dry-to-wet transition season (Espinoza et al. 2019). The enhancement of dry conditions is also reflected by the reductions of river discharge of the southern Amazon tributaries, mainly during the low-water season (Espinoza et al. 2009; Lopes et al. 2016; Molina-Carpio et al. 2017). In addition, recent studies have detected a higher frequency of dry-regime atmospheric patterns during the dry-to-wet transition season over the southern Amazon,

favoring a delayed monsoon and anomalous dry conditions over the region (Espinoza et al. 2021). Changes in thermodynamic stability through the atmospheric column and cold air incursions are also related to variations of the wet season onset in the Amazon (Li and Fu 2006; Nieto-Ferreira et al. 2011; Yin et al. 2014). Land cover changes over the southern Amazon have been highlighted as a possible cause of the observed lengthening of the southern Amazon dry season (Costa and Pires 2010; Alves et al. 2017; Agudelo et al. 2019; Ruiz-Vásquez et al. 2020). Moreover, projections under different GHG concentration scenarios indicate: (1) an increased duration of the dry season over the southern Amazon according to CMIP5 (Fu et al. 2013; Boisier et al. 2015) and CMIP6 models (Sena and Magnusdottir 2020; Wainwright et al. 2021, 2022), (2) an increased dry-day frequency (Arias et al. 2021a), and (3) an increased likelihood of droughts during the twenty-first century (Cook et al. 2020; Parsons 2020; Seneviratne et al. 2021). Although it was not possible to analyze the CMIP6 output regarding moisture transport, this consistency suggests that the results obtained in the present study are expected to be generally applicable. Nevertheless, future work should exploit the CMIP6 dataset, including high-resolution models to confirm these findings.

The projections discussed here correspond to a "worse" case emission scenario depicted by the RCP8.5 (Riahi et al. 2011). Mu et al. (2021) show that the atmospheric moisture supply from forests mitigate drought in the Brazilian Amazon, although this mechanism can be compensated due to circulation changes (Mu et al. 2023). Thus, considering the land cover change used by the RCP8.5, the projection of reductions in the contributions to P from the main atmospheric moisture sources, the reductions of total P, and the reductions of recycled P over the Amazon during the dry season could be linked to land cover and atmospheric transport changes.

The analysis presented here contributes to provide further elements in the understanding of the observed and projected changes in the hydroclimatology of the southern Amazon by analyzing simulations of variables that are better represented by models, such as PW and atmospheric moisture transport. Recently, Olmo et al. (2022) identified that to study the monsoon timing, and therefore changes during the dry and the dry-to-wet transition seasons in the southern Amazon, using General Circulation Models (GCMs), may be more appropriate to analyze dynamic variables related to atmospheric circulation. Likewise, our study relies on the complementary analysis of atmospheric moisture transport, an aspect deeply associated with regional atmospheric circulation, to understand hydroclimatic changes over tropical South America, especially the Amazon. This may be a useful way to take a major advantage of GCM simulations in order to understand the possible effects of global climate change at regional scale.

Declarations

Conflict of interest The authors declare no conflicts of interest or competing interests.

Ethical approval Not applicable.

References

Agudelo J, Arias PA, Vieira SC et al (2019) Influence of longer dry seasons in the southern Amazon on patterns of water vapor transport over northern South America and the Caribbean. Clim Dyn 52(5–6):2647–2665. https://doi.org/10.1007/s00382-018-4285-1

Allan RP, Barlow M, Byrne MP, Cherchi A et al (2020) Advances in understanding large-scale responses of the water cycle to climate change. Ann N Y Acad Sci 1472:49–75. https://doi.org/10.1111/nyas.14337

Allan RP, Willett KM, John VO, Trent T (2022) Global changes in water vapor 1979–2020. J Geophys Res Atmos 127:e2022JD036728. https://doi.org/10.1029/2022JD036728

Alves LM, Marengo JA, Fu R, Bombardi RJ (2017) Sensitivity of Amazon regional climate to deforestation. Am J Clim Change 6(01):75–98

Ampuero A, Stríkis NM, Apaéstegui J, Vuille M, Novello VF, Espinoza JC, Sifeddine A (2020) The forest effects on the isotopic composition of rainfall in the northwestern Amazon basin. J Geophys Res Atmos 125:e2019JD031445. https://doi.org/10.1029/2019jd031445

Arias PA, Fu R, Vera C, Rojas M (2015a) A correlated shortening of the North and South American monsoon seasons in the past few decades. Clim Dyn 45(11–12):3183–3203. https://doi.org/10.1007/s00382-015-2533-1

Arias PA, Martínez JA, Vieira SC (2015b) Moisture sources to the 2010–2012 anomalous wet season in northern South America. Clim Dyn 45(9–10):2861–2884. https://doi.org/10.1007/s00382-015-2511-7

Arias PA, Martínez JA, Mejía JD, Pazos MJ, Espinoza JC, Wongchui-Correa S (2020) Changes in Normalized Difference Vegetation Index in the Orinoco and Amazon River basins: links to tropical Atlantic surface temperatures. J Clim 33(19):8537–8559. https://doi.org/10.1175/JCLI-D-19-0696.1

Arias PA, Bellouin N, Coppola E et al (2021a) Technical summary. In: Masson-Delmotte V, Zhai P, Pirani A, Connors SL, Péan C, Berger S, Caud N, Chen Y, Goldfarb L, Gomis MI, Huang M, Leitzell K, Lonnoy E, Matthews JBR, Maycock TK, Waterfield T, Yelekçi O, Yu R, Zhou B (eds) Climate change 2021: the physical science basis. Contribution of working group I to the sixth assessment report of the intergovernmental panel on climate change. Cambridge University Press, Cambridge, pp 33–144

Arias PA, Ortega G, Villegas LD, Martínez JA (2021b) Colombian climatology in CMIP5/CMIP6 models: persistent biases and improvements. Rev Facul Ingeniería Univ Antioquia 100:75–96. https://doi.org/10.17533/udea.redin.20210525

Arora VK, Scinocca JF, Boer GJ et al (2011) Carbon emission limits required to satisfy future representative concentration pathways of greenhouse gases. Geophys Res Lett 38(5):L05805. https://doi.org/10.1029/2010GL046270

Artaxo P, Almeida-Val VMF, Bilbao B, Brando P, Bustamante M, Coe MT, Correa SB, Cuesta F, Costa MH, Miralles-Wilhelm F, Salinas N, Silvério DV, Val AL (2021) Chapter 23: Impacts of deforestation and climate change on biodiversity, ecological processes, and environmental adaptation. In: Nobre C, Encalada A, Anderson E, Roca Alcazar FH, Bustamante M, Mena C, Peña-Claros M, Poveda G, Rodriguez JP, Saleska S, Trumbore S, Val AL, Villa Nova L, Abramovay R, Alencar A, Rodríguez Alzza C, Armenteras D, Artaxo P, Athayde S, Barretto Filho HT, Barlow J, Berenguer E, Bortolotto F, Costa FA, Costa MH, Cuvi N, Fearnside PM, Ferreira J, Flores BM, Frieri S, Gatti LV, Guayasamin JM, Hecht S, Hirota M, Hoorn C, Josse C, Lapola DM, Larrea C, Larrea-Alcazar DM, Lehm Ardaya Z, Malhi Y, Marengo JA, Melack J, Moraes RM, Moutinho P, Murmis MR, Neves EG, Paez B, Painter L, Ramos A, Rosero-Peña MC, Schmink M, Sist P, ter Steege H, Val P, van der Voort H, Varese M, Zapata-Ríos G (eds) Amazon assessment report 2021. United Nations Sustainable Development Solutions Network, New York. https://doi.org/10.55161/VKMN1905

Boisier JP, Ciais P, Ducharne A, Guimberteau M (2015) Projected strengthening of Amazonian dry season by constrained climate model simulations. Nat Clim Chang 5(7):656–660. https://doi.org/10.1038/nclimate2658

Bonilla-Ovallos CA, Mesa-Sánchez OJ (2017) Validación de la precipitación estimada por modelos climáticos acoplados del proyecto de intercomparación CMIP5 en Colombia. Rev Acad Colomb Cienc Exact Físic Nat 41(158):107. https://doi.org/10.18257/raccefyn.427

Bosilovich MG, Chern J-D (2006) Simulation of Water Sources and Precipitation Recycling for the MacKenzie, Mississippi, and Amazon River Basins. J Hydrometeorol 7(3):312–329. https://doi.org/10.1175/JHM501.1

Byrne MP, O'Gorman PA (2018) Trends in continental temperature and humidity directly linked to ocean warming. PNAS 115:4863–4868

Castellanos E, Lemos MF, Astigarraga L et al (2022) Central and South America. In: Pörtner H-O, Roberts DC, Tignor M, Poloczanska ES, Mintenbeck K, Alegría A, Craig M, Langsdorf S, Löschke S, Möller V, Okem A, Rama B (eds) Climate change 2022: impacts,

adaptation, and vulnerability. Contribution of working group II to the sixth assessment report of the intergovernmental panel on climate change. Cambridge University Press, Cambridge (**in press**)

Ceglar A, Toreti A, Balsamo G, Kobayashi S (2017) Precipitation over monsoon Asia: a comparison of Reanalyses and Observations. J Clim 30(2):465–476. https://doi.org/10.1175/JCLI-D-16-0227.1

Cintra BBL, Gloor M, Boom A et al (2022) Tree-ring oxygen isotopes record a decrease in Amazon dry season rainfall over the past 40 years. Clim Dyn 59:1401–1414. https://doi.org/10.1007/s00382-021-06046-7

Cook BI, Mankin JS, Marvel K, Williams AP, Smerdon JE, Anchukaitis KJ (2020) Twenty-first century drought projections in the CMIP6 forcing scenarios. Earth's Future 8:e2019EF001461. https://doi.org/10.1029/2019EF001461

Correa I, Arias PA, Rojas M (2021) Evaluation of multiple indices of the South American monsoon. Int J Climatol 41:E2801–E2819. https://doi.org/10.1002/joc.6880

Costa MH, Pires GF (2010) Effects of Amazon and Central Brazil deforestation scenarios on the duration of the dry season in the arc of deforestation. Int J Climatol 30(13):1970–1979

Debortoli N, Dubreuil V, Fanatsu B, Delahaye F, de Oliveira HC, Rodrigues-Filho S, Saito CH, Fetter R (2015) Rainfall patterns in the Southern Amazon: a chronological perspective (1971–2010). Clim Change 130:1573–1480. https://doi.org/10.1007/s10584-015-1415-1

Dirmeyer PA, Brubaker KL, DelSole T (2009) Import and export of atmospheric water vapor between nations. J Hydrol 365(1–2):11–22

Dirmeyer PA, Jin Y, Csingh C, Yan C (2013a) Evolving land-atmosphere interactions over North America from CMIP5 simulations. J Clim 26(19):7313–7327. https://doi.org/10.1175/JCLI-D-12-00454.1

Dirmeyer PA, Jin Y, Singh B, Yan X (2013b) Trends in land-atmosphere interactions from CMIP5 simulations. J Hydrometeorol 14(3):829–849. https://doi.org/10.1175/JHM-D-12-0107.1

Dominguez F, Kumar P, Liang XZ et al (2006) Impact of atmospheric moisture storage on precipitation recycling. J Clim 19(8):1513–1530. https://doi.org/10.1175/JCLI3691.1

Dominguez F, Hu H, Martinez JA (2020) Two-layer dynamic recycling model (2L-DRM): learning from moisture tracking models of different complexity. J Hydrometeorol 21(1):3–16

Dominguez F, Eiras-Barca J, Yang Z, Bock D, Nieto R, Gimeno L (2022) Amazonian moisture recycling revisited using WRF with water vapor tracers. J Geophys Res Atmos 127:e2021JD035259. https://doi.org/10.1029/2021JD035259

Donner LJ, Wyman BL, Hemler RS et al (2011) The dynamical core, physical parameterizations, and basic simulation characteristics of the atmospheric component AM3 of the GFDL global coupled model CM3. J Clim 24(13):3484–3519

Douville H, Raghavan K, Renwick J et al (2021) Water Cycle Changes. In: Masson-Delmotte V, Zhai P, Pirani A, Connors SL, Péan C, Berger S, Caud N, Chen Y, Goldfarb L, Gomis MI, Huang M, Leitzell K, Lonnoy E, Matthews JBR, Maycock TK, Waterfield T, Yelekçi O, Yu R, Zhou B (eds) Climate change 2021: the physical science basis. Contribution of working group I to the sixth assessment report of the intergovernmental panel on climate change. Cambridge University Press, Cambridge, pp 1055–1210

Drumond A, Nieto R, Gimeno L, Ambrizzi T (2008) A Lagrangian identification of major sources of moisture over Central Brazil and la Plata Basin. J Geophys Res Atmos. https://doi.org/10.1029/2007JD009547

Drumond A, Marengo J, Ambrizzi T, Nieto R, Moreira L, Gimeno L (2014) The role of the Amazon Basin moisture in the atmospheric branch of the hydrological cycle: a Lagrangian analysis.

Hydrol Earth Syst Sci 18(7):2577–2598. https://doi.org/10.5194/hess-18-2577-2014

Eiras-Barca J, Algarra I, Nieto R, Schröder M, Hegglin MI, Gimeno L (2022) Analysis of the main source regions of moisture transport events with the new ESA CCI/CM-SAF total column water vapour climate data record (v2). Q J R Meteorol Soc 148(748):3244–3258. https://doi.org/10.1002/qj.4358

Escobar M, Hoyos I, Nieto R, Villegas JC (2022) The importance of continental evaporation for precipitation in Colombia: a baseline combining observations from stable isotopes and modelling moisture trajectories. Hydrol Process 36(6):e14595. https://doi.org/10.1002/hyp.14595

Espinoza JC, Ronchail J, Guyot JL, Cochonneau G, Naziano F, Lavado W et al (2009) Spatio-temporal rainfall variability in the Amazon basin countries (Brazil, Peru, Bolivia, Colombia, and Ecuador). Int J Climatol 29(11):1574–1594. https://doi.org/10.1002/joc.1791

Espinoza JC, Ronchail J, Marengo JA, Segura H (2019) Contrasting North-South changes in Amazon wet-day and dry-day frequency and related atmospheric features (1981–2017). Clim Dyn 52(9–10):5413–5430. https://doi.org/10.1007/s00382-018-4462-2

Espinoza JC, Arias PA, Moron V, Junquas C, Segura H et al (2021) Recent changes in the atmospheric circulation patterns during the dry-to-wet transition season in south tropical South America (1979–2020): impacts on precipitation and fire season. J Clim 34(22):9025–9042. https://doi.org/10.1175/JCLI-D-21-0303.1

Essou GRC, Sabarly F, Lucas-Picher P, Brissette F, Poulin A (2016) Can precipitation and temperature from meteorological reanalyses be used for hydrological modeling? J Hydrometeorol 17(7):1929–1950. https://doi.org/10.1175/JHM-D-15-0138.1

Fu R, Yin L, Li W, Arias PA, Dickinson RE, Huang L et al (2013) Increased dry season length over southern Amazonia in recent decades and its implication for future climate projection. Proc Natl Acad Sci 110(45):18110–18115. https://doi.org/10.1073/pnas.1302584110

Gallego D, García-Herrera R, Gómez-Delgado FDP, Ordoñez-Perez P, Ribera P (2019) Tracking the moisture transport from the Pacific towards Central and northern South America since the late 19th century. Earth Syst Dyn 10(2):319–331

Gimeno L, Stohl A, Trigo RM, Dominguez F et al (2012) Oceanic and terrestrial sources of continental precipitation. Rev Geophys 50:RG4003. https://doi.org/10.1029/2012RG000389

Gimeno L, Dominguez F, Nieto R et al (2016) Major mechanisms of atmospheric moisture transport and their role in extreme precipitation events. Annu Rev Environ Resour 41(1):117–141

Gimeno L, Nieto R, Sorí R (2020) The growing importance of oceanic moisture sources for continental precipitation. Npj Clim Atmos Sci 3:27. https://doi.org/10.1038/s41612-020-00133-y

Giráldez L, Silva Y, Zubieta R, Sulca J (2020) Change of the rainfall seasonality over central peruvian andes: onset, end, duration and its relationship with large-scale atmospheric circulation. Climate 8:23. https://doi.org/10.3390/cli8020023

Goessling HF, Reick CH (2013) On the '"well-mixed"' assumption and numerical 2-D tracing of atmospheric moisture. Atmos Chem Phys 13:5567–5585. https://doi.org/10.5194/acp-13-5567-2013

Haghtalab N, Moore N, Heerspink BP, Hyndman DW (2020) Evaluating spatial patterns in precipitation trends across the Amazon basin driven by land cover and global scale forcings. Theoret Appl Climatol 140:411–427

Held IM, Soden BJ (2006) Robust responses of the hydrological cycle to global warming. J Clim 19(21):5686–5699. https://doi.org/10.1175/JCLI3990.1

Herrera-Estrada JE, Martinez JA, Dominguez F, Findell KL, Wood EF, Sheffield J (2019) Reduced moisture transport linked to

drought propagation across North America. Geophys Res Lett 46(10):5243–5253

Hersbach H, Bell B, Berrisford P, Hirahara S, Horányi A, Muñoz-Sabater J, Nicolas J, Peubey C, Radu R, Schepers D, Simmons A, Soci C, Abdalla S, Abellan X, Balsamo G, Bechtold P, Biavati G, Bidlot J, Bonavita M, De Chiara G, Dahlgren P, Dee D, Diamantakis M, Dragani R, Flemming J, Forbes R, Fuentes M, Geer A, Haimberger L, Healy S, Hogan RJ, Hólm E, Janisková M, Keeley S, Laloyaux P, Lopez P, Lupu C, Radnoti G, de Rosnay P, Rozum I, Vamborg F, Villaume S, Thépaut J-N (2020) The ERA5 global reanalysis. Q J R Meteorol Soc 146(730):1999–2049. https://doi.org/10.1002/qj.3803

Hirota N, Takayabu YN (2013) Reproducibility of precipitation distribution over the tropical oceans in CMIP5 multi-climate models compared to CMIP3. Clim Dyn 41(11–12):2909–2920. https://doi.org/10.1007/s00382-013-1839-0

Hoyos I, Dominguez F, Cañón-Barriga J, Martínez JA, Nieto R, Gimeno L, Dirmeyer PA (2018) Moisture origin and transport processes in Colombia, northern South America. Clim Dyn 50:971–990. https://doi.org/10.1007/s00382-017-3653-6

Hoyos I, Cañón-Barriga J, Arenas-Suárez T, Dominguez F, Rodríguez BA (2019) Variability of regional atmospheric moisture over Northern South America: patterns and underlying phenomena. Clim Dyn 52:893–911. https://doi.org/10.1007/s00382-018-4172-9

IPCC (2021) Summary for policymakers. In: MassonDelmotte V, Zhai P, Pirani A, Connors SL, Péan C, Berger S, Caud N, Chen Y, Goldfarb L, Gomis MI, Huang M, Leitzell K, Lonnoy E, Matthews JBR, Maycock TK, Waterfield T, Yelekçi O, Yu R, Zhou B (eds) Climate change 2021: the physical science basis. Contribution of working group I to the sixth assessment report of the intergovernmental panel on climate change. Cambridge University Press, Cambridge, pp 3–32. https://doi.org/10.1017/9781009157896.001

Joetzjer E, Douville H, Delire C, Ciais P (2013) Present-day and future Amazonian precipitation in global climate models: CMIP5 versus CMIP3. Clim Dyn 41(11–12):2921–2936. https://doi.org/10.1007/s00382-012-1644-1

Koster RD, Dirmeyer PA, Hahmann AN, Ijpelaar R, Tyahla L, Cox P, Suarez MJ (2002) Comparing the degree of land-atmosphere interaction in four atmospheric general circulation models 3(3):363–375. http://journals.ametsoc.org/jhm/article-pdf/3/3/363/4144983/1525-7541

Laîné A, Nakamura H, Nishii K, Miyasaka T (2014) A diagnostic study of future evaporation changes projected in CMIP5 climate models. Clim Dyn 42(9–10):2745–2761. https://doi.org/10.1007/s00382-014-2087-7

Lavers DA, Allan RP, Villarini G, Lloyd-Hughes B, Brayshaw DJ, Wade AJ (2013) Future changes in atmospheric rivers and their implications for winter flooding in Britain. Environ Res Lett. https://doi.org/10.1088/1748-9326/8/3/034010

Lavers DA, Ralph FM, Waliser DE, Gershunov A, Dettinger MD (2015) Climate change intensification of horizontal water vapor transport in CMIP5. Geophys Res Lett 42(13):5617–5625. https://doi.org/10.1002/2015GL064672

Levang SJ, Schmitt RW (2015) Centennial changes of the global water cycle in CMIP5 models. J Clim 28(16):6489–6502. https://doi.org/10.1175/JCLI-D-15-0143.1

Li W, Fu R (2006) Influence of cold air intrusions on the wet season onset over Amazonia. J Clim 19:257–275. https://doi.org/10.1175/JCLI3614.1

Liu C, Allan RP (2013) Observed and simulated precipitation responses in wet and dry regions 1850–2100. Environ Res Lett. https://doi.org/10.1088/1748-9326/8/3/034002

Lopes A, Chiang J, Thompson S, Dracup J (2016) Trend and uncertainty in spatial-temporal patterns of hydrological droughts in the Amazon basin. Geophys Res Lett 43(7):3307–3316

Lorenz R, Argüeso D, Donat MG, Pitman, et al (2016) Influence of land-atmosphere feedbacks on temperature and precipitation extremes in the GLACE-CMIP5 ensemble. J Geophys Res 121(2):607–623. https://doi.org/10.1002/2015JD024053

Marengo JA, Fisch GF, Alves LM, Sousa NV, Fu R, Zhuang Y (2017) Meteorological context of the onset and end of the rainy season in central Amazonia during the goAmazon2014/5. Atmos Chem Phys 17(12):7671–7681

Martínez JA, Dominguez F (2014) Sources of atmospheric moisture for the La Plata river basin. J Clim 27(17):6737–6753. https://doi.org/10.1175/JCLI-D-14-00022.1

Martins G, von Randow C, Sampaio G, Dolman AJ (2015) Precipitation in the Amazon and its relationship with moisture transport and tropical Pacific and Atlantic SST from the CMIP5 simulation. Hydrol Earth Syst Sci Discuss 12(1):671–704. https://doi.org/10.5194/hessd-12-671-2015

Molina RD, Salazar JF, Martínez JA, Villegas JC, Arias PA (2019) Forest-induced exponential growth of precipitation along climatological wind streamlines over the Amazon. J Geophys Res Atmos 124(5):2589–2599. https://doi.org/10.1029/2018JD029534

Molina-Carpio J, Espinoza JC, Vauchel P, Ronchail J, Gutierrez Caloir B, Guyot JL, Noriega L (2017) Hydroclimatology of the upper madeira river basin: spatio-temporal variability and trends. Hydrol Sci J 62(6):911–927

Morales JS, Arias PA, Martínez JA, Durán-Quesada AM (2020) The role of low-level circulation on water vapor transport to Central and northern South America: insights from a 2D Lagrangian approach. Int J Climatol 41(S1):E2662–E2682. https://doi.org/10.1002/joc.6873

Mu Y, Biggs TW, De Sales F (2021) Forests mitigate drought in an agricultural region of the Brazilian Amazon: atmospheric moisture tracking to identify critical source areas. Geophys Res Lett 48:e2020GL091380. https://doi.org/10.1029/2020GL091380

Mu Y, Biggs TW, Jones C (2023) Importance in shifting circulation patterns for dry season moisture sources in the Brazilian Amazon. Geophys Res Lett 50:e2023GL103167. https://doi.org/10.1029/2023gl103167

Nieto R, Cirica D, Vázquez M, Liberato MLR, Gimeno L (2019) Contribution of the main moisture sources to precipitation during extreme peak precipitation months. Adv Water Resour 131:103385. https://doi.org/10.1016/j.advwatres.2019.103385

Nieto-Ferreira R, Rickenbach TM, Wright EA (2011) The role of cold fronts in the onset of the monsoon season in the South Atlantic convergence zone. Q J R Meteorol Soc 137(657):908–922

O'Gorman PA, Muller CJ (2010) How closely do changes in surface and column water vapor follow Clausius-Clapeyron scaling in climate change simulations? Environ Res Lett. https://doi.org/10.1088/1748-9326/5/2/025207

Olmo ME, Espinoza JC, Bettolli ML, Sierra JP, Junquas C, Arias PA, Moron V, Balmaceda-Huarte R (2022) Circulation patterns and associated rainfall over South Tropical South America: GCMs evaluation during the dry-to-wet transition season. J Geophys Res Atmos 127(12):es2022JD036468. https://doi.org/10.1029/2022JD036468

Ortega G, Arias PA, Villegas JC, Marquet PA, Nobre P (2021) Present-day and future climate over Central and South America according to CMIP5/CMIP6 models. Int J Climatol 41(15):6713–6735. https://doi.org/10.1002/joc.7221

Palomino-Lemus R, Córdoba-Machado S, Gámiz-Fortis SR, Castro-Díez Y, Esteban-Parra MJ (2015) Summer precipitation projections over northwestern South America from CMIP5 models.

Glob Planet Change 131:11–23. https://doi.org/10.1016/j.glopl acha.2015.05.004

Palomino-Lemus R, Córdoba-Machado S, Gámiz-Fortis SR, Castro-Díez Y, Esteban-Parra MJ (2017) Climate change projections of boreal summer precipitation over tropical America by using statistical downscaling from CMIP5 models. Environ Res Lett 12(12):124011. https://doi.org/10.1088/1748-9326/aa9bf7

Parsons LA (2020) Implications of CMIP6 projected drying trends for 21st century Amazonian drought risk. Earth's Future 8:e2020EF001608. https://doi.org/10.1029/2020EF001608

Poveda G, Jaramillo L, Vallejo LF (2014) Seasonal precipitation patterns along pathways of South American low-level jets and aerial rivers. Water Resour Res 50(1):98–118

Riahi K, Rao S, Krey V, Cho C, Chirkov V, Fischer G, Rafaj P (2011) RCP 8.5—a scenario of comparatively high greenhouse gas emissions. Clim Change 109(1–2):33

Rocha VM, Correia FWS, da Silva PRT et al (2017) Reciclagem de precipitação na bacia amazônica: O papel do transporte de umidade e da evapotranspiração da superfície. Rev Bras Meteorol 32(3):387–398. https://doi.org/10.1590/0102-77863230006

Roy T, Martinez JA, Herrera-Estrada JE, Zhang Y, Dominguez F, Berg A, Wood EF (2019) Role of moisture transport and recycling in characterizing droughts: Perspectives from two recent US droughts and the CFSv2 system. J Hydrometeorol 20(1):139–154

Ruiz-Vásquez M, Arias PA, Martínez JA et al (2020) Effects of Amazon basin deforestation on regional atmospheric circulation and water vapor transport towards tropical South America. Clim Dyn 54(9):4169–4189. https://doi.org/10.1007/s00382-020-05223-4

Ruiz-Vásquez M, Arias PA, Martínez JA (2022) ENSO influence on water vapor transport and thermodynamics over Northern South America. Clim Dyn **(under review)**

Rusticucci M, Zazulie N, Raga GB (2014) Regional winter climate of the southern central Andes: assessing the performance of ERA-Interim for climate studies. J Geophys Res 119(14):8568–8582. https://doi.org/10.1002/2013JD021167

Ruv Lemes M, Sampaio G, Fisch G, Alves LM, Maksic J, Guatura M, Shimizu M (2023) Impacts of atmospheric CO_2 increase and Amazon deforestation on the regional climate: a water budget modelling study. Int J Climatol 43(3):1497–1513. https://doi.org/10.1002/joc.7929

Sakamoto MS, Ambrizzi T, Poveda G (2011) Moisture sources and life cycle of convective systems over Western Colombia. Adv Meteorol 2011:1–11. https://doi.org/10.1155/2011/890759

Sampaio G, Shimizu MH, Guimarães-Júnior CA, Alexandre F, Guatura M, Cardoso M, Domingues TF, Rammig A, von Randow C, Rezende LFC, Lapola DM (2021) CO_2 physiological effect can cause rainfall decrease as strong as large-scale deforestation in the Amazon. Biogeosciences 18:2511–2525. https://doi.org/10.5194/bg-18-2511-2021

Satyamurty P, da Costa CPW, Manzi AO (2013) Moisture source for the Amazon Basin: a study of contrasting years. Theor Appl Climatol 111(1–2):195–209. https://doi.org/10.1007/s00704-012-0637-7

Sena ACT, Magnusdottir G (2020) Projected end-of-century changes in the South American monsoon in the CESM large ensemble. J Clim 33(18):7859–7874. https://doi.org/10.1175/JCLI-D-19-0645.1

Seneviratne SI, Zhang X, Adnan M et al (2021) Weather and climate extreme events in a changing climate. In: Masson-Delmotte V, Zhai P, Pirani A, Connors SL, Péan C, Berger S, Caud N, Chen Y, Goldfarb L, Gomis MI, Huang M, Leitzell K, Lonnoy E, Matthews JBR, Maycock TK, Waterfield T, Yelekçi O, Yu R, Zhou B (eds) Climate change 2021: the physical science basis. Contribution of working group I to the sixth assessment report of the intergovernmental panel on climate change. Cambridge

University Press, Cambridge, pp 1513–1766. https://doi.org/10.1017/9781009157896.013

Serreze MC, Hurst CM (2000) Representation of mean arctic precipitation from NCEP-NCAR and ERA reanalyses 13(1):182–201. https://doi.org/10.1175/1520-0442(2000)0132.0.CO;2

Sierra JP, Arias PA, Vieira SC (2015) Precipitation over northern South America and its seasonal variability as simulated by the CMIP5 models. Adv Meteorol 2015:1–22. https://doi.org/10.1155/2015/634720

Sierra JP, Arias PA, Vieira SC, Agudelo J (2018) How well do CMIP5 models simulate the low-level jet in western Colombia? Clim Dyn 51(5–6):2247–2265

Sörensson AA, Ruscica RC (2018) Intercomparison and uncertainty assessment of nine evapotranspiration estimates over South America. Water Resour Res 54(4):2891–2908. https://doi.org/10.1002/2017WR021682

Sorí R, Marengo JA, Nieto R, Drumond A, Gimeno L (2018) The atmospheric branch of the hydrological cycle over the Negro and Madeira River Basins in the Amazon Region. Water 10(6):738. https://doi.org/10.3390/w10060738

Staal A, Tuinenburg OA, Bosmans JHC et al (2018) Forest-rainfall cascades buffer against drought across the Amazon. Nat Clim Change 8:539–543. https://doi.org/10.1038/s41558-018-0177-y

Stohl A, James P (2004) A Lagrangian analysis of the atmospheric branch of the global water cycle. Part I: method description, validation, and demonstration for the August 2002 flooding in central Europe. J Hydrometeorol 5(4):656–678

Swann AL, Longo M, Knox RG, Lee E, Moorcroft PR (2015) Future deforestation in the Amazon and consequences for South American climate. Agric Meteorol 214:12–24

Taylor KE (2001) Summarizing multiple aspects of model performance in a single diagram. J Geophys Res Atmos 106(D7):7183–7192. https://doi.org/10.1029/2000JD900719

Taylor KE, Stouffer RJ, Meehl GA (2012) An overview of CMIP5 and the experiment design. Bull Am Meteorol Soc 93(4):485–498

Tian B, Dong X (2020) The double-ITCZ bias in CMIP3, CMIP5, and CMIP6 models based on annual mean precipitation. Geophys Res Lett 47(8):e2020GL087232. https://doi.org/10.1029/2020GL087232

Torres RR, Marengo JA (2014) Climate change hotspots over South America: from CMIP3 to CMIP5 multi-model datasets. Theor Appl Climatol 117:579–587. https://doi.org/10.1007/s00704-013-1030-x

Trenberth KE (2011) Changes in precipitation with climate change. Clim Res 47(1–2):123–138. https://doi.org/10.3354/cr00953

Tuinenburg OA, Staal A (2020) Tracking the global flows of atmospheric moisture and associated uncertainties. Hydrol Earth Sys Sci 24(5):2419–2435. https://doi.org/10.5194/hess-24-2419-2020

Tuinenburg OA, Theeuwen JJE, Staal A (2020) High-resolution global atmospheric moisture connections from evaporation to precipitation. Earth Syst Sci Data 12(4):3177–3188. https://doi.org/10.1594/PANGAEA.912710

Wainwright CM, Black E, Allan RP (2021) Future changes in wet and dry season characteristics in CMIP5 and CMIP6 simulations. J Hydrometeorol 22(9):2339–2357. https://doi.org/10.1175/JHM-D-21-0017.1

Wainwright CM, Allan RP, Black E (2022) Consistent trends in dry spell length in recent observations and future projections. Geophys Res Lett 49:e2021GL097231. https://doi.org/10.1029/2021GL097231

Warner MD, Mass CF, Salathé EP (2015) Changes in winter atmospheric rivers along the North American west coast in CMIP5 climate models. J Hydrometeorol 16(1):118–128. https://doi.org/10.1175/JHM-D-14-0080.1

Watanabe M, Suzuki T, O'ishi R et al (2010) Improved climate simulation by MIROC5: mean states, variability, and climate sensitivity. J Clim 23(23):6312–6335

Watters D, Battaglia A, Allan RP (2021) The diurnal cycle of precipitation according to multiple decades of global satellite observations, three CMIP6 models, and the ECMWF reanalysis. J Clim 34(12):5063–5080. https://doi.org/10.1175/jcli-d-20-0966.1

Willett KM, Dunn RJH, Thorne PW, Bell S, de Podesta M, Parker DE et al (2014) HadISDH land surface multi-variable humidity and temperature record for climate monitoring. Clim past 10(6):1983–2006. https://doi.org/10.5194/cp-10-1983-2014

Willett KM, Dunn RJH, Kennedy JJ, Berry DI (2020) Development of the HadISDH marine humidity climate monitoring data set. Earth Syst Sci Data 12(4):2853–2880. https://doi.org/10.5194/essd-12-2853-2020

Xu H, Lian X, Slette IJ, Yang H, Zhang Y, Chen A, Piao S (2022) Rising ecosystem water demand exacerbates the lengthening of tropical dry seasons. Nat Commun 13(1):4093. https://doi.org/10.1038/s41467-022-31826-y

Yang Y, Liu C, Ou N, Liao X, Cao N, Chen N, Jin L, Zheng R, Yang K, Su Q (2022) Moisture transport and contribution to the continental precipitation. Atmosphere 13(10):1694. https://doi.org/10.3390/atmos13101694

Yin L, Fu R, Shevliakova E, Dickinson RE (2013) How well can CMIP5 simulate precipitation and its controlling processes over tropical South America? Clim Dyn 41(11–12):3127–3143. https://doi.org/10.1007/s00382-012-1582-y

Yin L, Fu R, Zhang Y, Arias PA et al (2014) What controls interannual variations of the wet season onsets over the Amazon? J Geophys Res 119(5):2314–2328. https://doi.org/10.1002/2013JD021349

Yukimoto S, Adachi Y, Hosaka M (2012) A new global climate model of the Meteorological Research Institute: MRI-CGCM3—model description and basic performance. J Meteorol Soc Jpn Ser II 2 90:23–64

Zahn M, Allan RP (2013) Quantifying present and projected future atmospheric moisture transports onto land. Water Resour Res 49:7266–7277. https://doi.org/10.1002/2012WR013209

Zanchettin D, Rubino A, Matei D, Bothe O, Jungclaus JH (2013) Multidecadal-to-centennial SST variability in the MPI-ESM simulation ensemble for the last millennium. Clim Dyn 40(5–6):1301–1318

Zemp DC, Schleussner CF, Barbosa HMJ, Van Der Ent RJ, Donges JF, Heinke J, Sampaio G, Rammig A (2014) On the importance of cascading moisture recycling in South America. Atmos Chem Phys 14(23):13337–13359. https://doi.org/10.5194/acp-14-13337-2014

Zhang ZS, Nisancioglu K, Bentsen M et al (2012) Pre-industrial and mid-Pliocene simulations with NorESM-L. Geosci Model Dev 5(2):523–533

Zhang X, Liu H, Zhang M (2015) Double ITCZ in coupled ocean-atmosphere models: from CMIP3 to CMIP5. Geophys Res Lett 42(20):8651–8659. https://doi.org/10.1002/2015GL065973

Zhang P, Chen G, Ma W, Ming Y, Wu Z (2021) Robust atmospheric river response to global warming in idealized and comprehensive climate models. J Clim 34(18):7717–7734. https://journals.ametsoc.org/view/journals/clim/34/18/JCLI-D-20-1005.1.xml

Zhou S, Huang G, Huang P (2020) Excessive ITCZ but negative SST biases in the tropical pacific simulated by CMIP5/6 models: the role of the meridional pattern of SST bias. J Clim 33(12):5305–5316. https://doi.org/10.1175/jcli-d-19-0922.1